processes

MDPI

Review

Biosensing on the Centrifugal Microfluidic Lab-on-a-Disc Platform

Celina M. Miyazaki [1,*], Eadaoin Carthy [2] and David J. Kinahan [2]

[1] Centre of Science and Technology for Sustainability, Federal University of Sao Carlos, Sorocaba, Sao Paulo 18052-780, Brazil

[2] School of Mechanical and Manufacturing Engineering, Dublin City University, Glasnevin, Dublin 9, Ireland; eadaoin.carthy@dcu.ie (E.C.); david.kinahan@dcu.ie (D.J.K.)

* Correspondence: celinamiyazaki@ufscar.br or celinammiyazaki@gmail.com

Received: 17 September 2020; Accepted: 22 October 2020; Published: 28 October 2020

Abstract: Lab-on-a-Disc (LoaD) biosensors are increasingly a promising solution for many biosensing applications. In the search for a perfect match between point-of-care (PoC) microfluidic devices and biosensors, the LoaD platform has the potential to be reliable, sensitive, low-cost, and easy-to-use. The present global pandemic draws attention to the importance of rapid sample-to-answer PoC devices for minimising manual intervention and sample manipulation, thus increasing the safety of the health professional while minimising the chances of sample contamination. A biosensor is defined by its ability to measure an analyte by converting a biological binding event to tangible analytical data. With evolving manufacturing processes for both LoaDs and biosensors, it is becoming more feasible to embed biosensors within the platform and/or to pair the microfluidic cartridges with low-cost detection systems. This review considers the basics of the centrifugal microfluidics and describes recent developments in common biosensing methods and novel technologies for fluidic control and automation. Finally, an overview of current devices on the market is provided. This review will guide scientists who want to initiate research in LoaD PoC devices as well as providing valuable reference material to researchers active in the field.

Keywords: biosensors; LoaD platforms; microfluidics; centrifugal microfluidics; PoC devices

1. Introduction

The development of microfluidic biosensors with rapid, sensitive, and selective response has been the focus of many research laboratories. Biosensors can be focused both on the clinical diagnosis of silent diseases, such as cancer, to guarantee that the patient is referred to as quickly as possible to the appropriate treatment, and in the routine control of chronic diseases such as diabetes, to give a rapid and easy indication of the medication dosage. Biosensors are defined by the International Union of Pure and Applied Chemistry (IUPAC) as "a device that uses specific biochemical reactions mediated by isolated enzymes, immunosystems, tissues, organelles or whole cells to detect chemical compounds usually by electrical, thermal or optical signals" [1]. The biomolecule responsible for the analyte recognition is denoted as the biorecognition element [2], and is the key for the specificity of the biosensor. Since 2010, about 28,000 articles have been published in accordance with ISI of knowledge (Web of Science) with the topic "biosensors" (black bars on Figure 1A). Biosensors exhibit advantages over the traditional analytical methods including low-cost of manufacture, fast response time, easy handling (does not demand trained operators), portability, better batch-to-batch reproducibility, and often have comparable sensitivity and selectivity. Despite this, few biosensors have been commercialised due to the challenges with translating laboratory-based platforms to devices and instruments suitable for widespread application in practical situations.

Sample preparation is a critical step in ensuring that a biosensor can meet the required sensitivity and specificity. Sample preparation is often an arduous and labour-intensive task involving a range of laboratory unit operations (LUOs) such as metering, mixing, separation, resuspension, and elution. The versatility and usefulness of a biosensor is greatly reduced if sample preparation must be performed manually. Therefore, much effort has been made to encapsulate biosensors within microfluidic devices, or Lab-on-a-Chip devices, which can fully automate the required LUOs and therefore offer sample-to-answer performance. Microfluidics is related to the science and technology of systems that process or manipulates small amounts of fluids [3,4]. Biosensors based on microfluidic technology can offer reduced reagent volumes, reduced sample volume, increased automation, and can function without requiring expensive and large instrumentation. These advantages, combined with the potential for mass manufacturing, can lead to low-cost tests and can prevent sample and operator contamination by minimising the user intervention [5]. The combination of "biosensors" and "microfluidics" has been a consistent focus of the research community as shown in Figure 1A (connected blue squares).

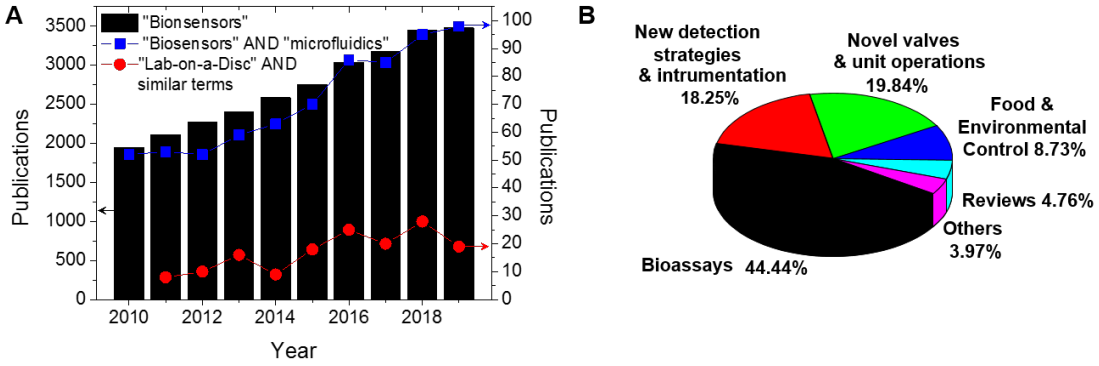

Figure 1. Web of Science results analysis by publication year using the topic (**A**) "biosensors" (black bars), the combination of "biosensors" and "microfluidics" (connected blue squares), and the terms "lab-on-a-disc" or "lab-on-a-CD" or "bio-disk" or "lab-CD" or "lab-disc" (connected red circles). (**B**) "lab-on-a-disc" results distributed in applications focus. Data from Clarivate Analytics (ISI Web of Knowledge [6]) in 18 May 2020.

Flow control (via pumping and valving) is a critical technology for enabling microfluidic systems. Prior to undertaking the design and fabrication of LoaD technology, it is important to understand non-centrifugally induced fluid flow mechanisms. Many methods of fluid manipulation and delivery have been reported. Passively driven microfluidics is a popular method as it is operated without an external fluid delivery system or actuator. Techniques such as osmosis [7,8], capillary action [9], pressure [10], gravity-driven flow [11], surface tension [12], vacuum-driven pressure [13], and hydrostatic flow [14] techniques can all be applied to achieve adequate fluid flow within microchannels. Applying these methods to microfluidic devices creates a robust, self-sufficient platform which can be utilised in any POC setting. Applying external triggers can further the capabilities of the devices and incorporates a variety of active driven device techniques. Manipulating fluid using an external trigger can allow for more complicated assays to be carried out in situ. Active fluid flow methods include electroosmotic [15], acoustic [16], photo-actuated [17], and pumping [18]. Both passive and active pumping mechanisms are important in understanding the dynamics of microfluidic devices. These methods may also be applied to centrifugal devices and can be amalgamated to create highly comprehensive POC tools. Centrifugal platforms can incorporate both types of fluid flow techniques; however, centrifugal forces play the main role of fluid displacement within the platform architecture. The Lab-on-a-Disc (LoaD) platform uses a typically disc-shaped cartridge and the pumping is via the centrifugal force; the disc-shaped chip is rotated about its axis. The general advantages of polymer chip-based microfluidics are that (i) mass production is possible with non-expensive infrastructure and

common polymers; (ii) low-cost acrylics or thermoplastics have replaced glass for chip production, and, therefore, the cost per unit is significantly reduced compared to other in vitro diagnostic (IVD) tests [19]; aside from those advantages, the LoaD systems present particular advantages, specifically that (i) the fluidic propulsion depends only on a low-cost and controllable spinning motor, without the need of pneumatic interfaces and pumps; (ii) liquid handling is widely independent of the sample properties, i.e., pH or ionic strength (pivotal for electrokinectic-based methods); (iii) possible full integration, automation, and miniaturisation are possible; and (iv) there is possible large-scale parallelisation and multiplexing of bioanalytical assays. Because of the optical transparency of polymer LoaDs and the no-contact nature of the detection set-up, the optical detection has been the most common approach in LoaD biosensors. Expertise developed in manufacture in disc-based storage media (Compact Disc ™ and Digital Versatile Disc ™) provides a strong knowledge base to support process development for manufacture of LoaDs. Figure 1A (connected red circles) illustrates the number of publications concerning LoaD platforms. Because different terms have been used in the literature, the search was made using "Lab-on-a-disc" OR "lab-on-a-CD" OR "Bio-disk" OR "Lab-disc" OR "Lab-CD" as topic keywords. The number of publications are generally trending upwards demonstrating an increased interest in the LoaD platform while the variability in the trend likely reflects that LoaD remains a niche platform. The application focus distribution of LoaD publications is shown in Figure 1B.

Recent developments in microfluidic research has allowed for the integration of well-established detection methods, such as optical or electrochemical, to create robust platforms capable of a sample-to-answer within a significantly reduced time [20]. The use of centrifugal microfluidic platforms allows for complex and automated sample handling integrated within the microfluidic chip. Alongside the favourable features listed above, a key advantage of the LoaD platform is the capability to apply centrifugation to the preparation of the sample for the biosensor. This is particularly useful when processing complex sample matrices such as whole blood; here, for example, it can be separated into its constituent components (plasma, red blood cells, and white blood cells) in a single step [21]. Furthermore, the reduced costs of micro-processors has also resulted in the emerging area of electronic LoaDs (eLoaD) where the instrumentation required by the biosensor can be miniaturised into a support instrument and, in some cases, can co-rotate with the LoaD. This allows for detection and analysis of biomolecules with significantly reduced data acquisition times [22]. Contextualising, for the majority of electrochemical-LoaDs, the electrodes are integrated onto the platform to connect the biosensors to the instrumentation while the electrochemical readouts are often made from a stationary disc [23,24]. Recently, measurements during disc rotation were enabled by electrical slip-rings [25] or, where the high background electrical noise associated with some slip-rings may greatly interfere with the electrical readout signal, using integrated micro-controllers with wireless data transfer [26,27].

Lab-on-a-Chip platforms (which are often called micro total analysis systems (μTAS)) that are based on LoaD platform are particularly suitable for point-of-care (PoC) diagnostics in low-resource settings. Application of these platforms in poor and remote areas is termed extreme point-of-care [28]. Guidance from the World Health Organization (WHO) recommends that the development of diagnostic tests to resource-limited settings should follow the ASSURED (Affordable, Sensitive, Specific, User-friendly, Rapid/Robust, Equipment-free, Deliverable) criteria [29,30]. An updated acronym was proposed in 2019 as REASSURED, with the inclusions of R as Real-time connectivity and E as Ease of specimen collection and Environmental friendliness [31]. Researchers have made great efforts to meet all these criteria but challenges still remain [19,28,32]. Certainly, centrifugal microfluidics has features which position it as the ideal platform for PoC diagnostic testing and is, therefore, at the forefront of extreme PoC device development.

The existing academic literature contains a number of well-regarded review papers addressing both the general LoaD platform and specific aspects of this technology platform [5,28,33–39]. In this review, we discuss the recent advances in centrifugal microfluidics focusing on biosensing applications. We tried to concentrate our discussion (but do not limit) in the literature over the past 10 years. We divide this paper into sections concerning the main protocols in biosensors. We aim to provide an

accessible guide for the ample audience of biosensor researchers with interest in leveraging LoaD technology to enhance their existing research while also providing a valuable resource for microfluidic specialists. Section 2 introduces the fluidic control in LoaD biosensors. Section 3 discusses the LoaD manufacture pointing both polymer microfabrication and biorecognition element immobilisation strategies. Section 4 describes the essential processing in LoaD biosensors while Section 5 discusses the existing and emerging LoaD PoC devices. We finalised with future perspectives and our final remarks in Sections 6 and 7, respectively.

2. Fluidic Control in LoaD Biosensors

The main driven-force in LoaD biosensors is the centrifugal force which acts outwards from the centre of rotation. Other pseudo-forces which play a role are the Coriolis force (applied when a particle/fluid moves in a rotating reference frame) and Euler force (induced by accelerating or decelerating the disc rotation). A combination of channel design, capillary action, and the placement of valves control can control the movement and timing of fluid movement. When a disc spins, the centrifugal force induces fluid flow radially outwards from the centre to the edge of the disc. Considering a fluid of mass density ρ on a planar disc rotating at a distance r from the central axis at an angular velocity ω, this liquid experiences a centrifugal force f_ω (Equation (1)) [34,35,40]

$$f_\omega = \rho r \omega^2 \tag{1}$$

a Euler force f_E given by Equation (2) [34,35]

$$f_E = \rho r \frac{d\omega}{dt} \tag{2}$$

with a rotational acceleration $\frac{d\omega}{dt}$, and a Coriolis force f_C (Equation (3)) [34,35,40]

$$f_C = 2\rho\omega v \tag{3}$$

where v is the fluid velocity in the plane. These three forces are represented in Figure 2, and can be controlled by the frequency of the rotation ω [35]. The centrifugal force induces the fluid to flow radially outward from the centre of the disc to the outer circumference [40]. The Coriolis force depends on the direction of rotation. If the direction changes, the direction of the Coriolis force changes [41]. It can be applied to mixing of samples, for flow switching, or directing of sample in specific channels [40]. In the "shake-mode" with continuous change in the spin speed, the angular momentum caused by the acceleration and deceleration induces Euler forces, resulting in a layer inversion of the fluid in the microfluidic chamber [34].

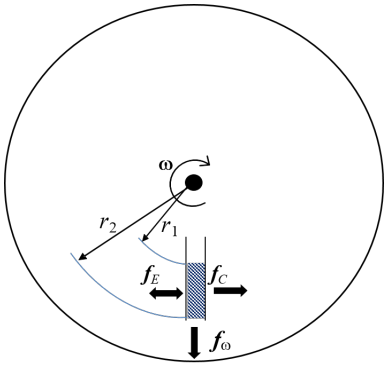

Figure 2. Forces acting in centrifugal microfluidics. The centrifugal force f_ω acts radially outward, the Coriolis force f_C acts perpendicular to ω and fluid speed, and the Euler force f_E is proportional to the angular acceleration.

The centrifugal flow rate depends on the rotational speed, radial location of the fluid reservoirs, channel geometry, and fluid properties such as viscosity, density, etc. [36]. Physicochemical properties as pH and ionic strength have no significant influence on the centrifugal flow rate, making it possible to pump many different fluids and integrate various processes on the same disc.

In a non-rotating reference frame under gravity (i.e., on the surface of the earth), the hydrostatic pressure is defined by the simple equation $\Delta P = \rho g h$ where g is the acceleration due to gravity and h is the height of the fluid column. Analogously, the centrifugally induced hydrostatic pressure is dependent on the radially inward and radially outward locations of a liquid columm on the disc (defined by r_1 and r_2 respectively in Figure 2). The centrifugally induced pressure, ΔP_c is defined as

$$\Delta P_c = \rho \omega^2 (\frac{r_2^2 - r_1^2}{2}) \quad (4)$$

In literature, this equation is commonly represented in an alternative form

$$\Delta P_c = \rho \omega^2 \Delta r \bar{r} \quad (5)$$

where Δr is the radial height of the liquid column ($\Delta r = r_2 - r_1$) and $\bar{r}$ is the radial center of the liquid column ($\bar{r} = \frac{(r_2 - r_1)}{2}$) [5].

While rotating, the centrifugal force acts on all liquids present on the disc and, therefore, to automate common assays, valves are required. Valves act just like faucets that control if and when the channels will deliver the fluid. Different types of valves have been proposed in the past years ranging from simple designs to highly sophisticated implementations. On the LoaD valves are typically "normally closed" (NC) such that in their initial state, they are closed and will open with some stimulus. Valves can also be "normally open" (NO), but these are less common and useful on LoaD. Most valves are classified as "single use" (i.e., changing from closed state to open state), but others can be changed between open and closed states. Valves are also classified as rationally-actuated or instrument-actuated [42]. Rotationally-actuated valves (also called passive valves) are controlled by changes in the disc spin rate (centrifugal force) while instrument-actuated valves (also called active valves) use an external actuator or source of energy (e.g., a laser, a pneumatic pump, a robotic arm) to control on-disc valves. The different types of valves and flow control techniques have recently been thoroughly reviewed [34,43]. However, here, we will introduce some of the most common and relevant valves to demonstrate how they are key components in the integration and parallelisation of bio-analytical processes on LoaD platform.

Capillary valves (see Figure 3A) are based on the balance between the capillary pressure and the centrifugally induced pressure [36]. In a common configuration, the capillary burst valve is connected to a reservoir through a straight channel, and when the disk is at rest or in low rotation speed, the liquid flows to fill the hydrophilic channel. However, it stops at the inlet of a suddenly expanded valve due to the capillary pressure [44], so the liquid will pass through a capillary valve only when the centrifugal force is high enough to break the capillary barrier pressure. In the hydrophobic valve (Figure 3B), hydrophobic regions in the microchannel prevent the fluidic movement. The valve opens when the centrifugal force overcomes a certain critical value [34,36]. In a siphon valve (Figure 3C), the disc is rotating in a high speed and the centrifugal force keeps prevents priming (via capillary pumping) of the siphon. With the decrease of the rotation speed, the siphon's hydrophilic channel is primed by the capillary force (acting against the direction of the centrifugal force). The liquid in the siphon is pumped by the capillary force over the siphon crest and radially outwards until the liquid meniscus passes the radial inward location of the liquid column (i.e., location r_1 described in Figure 2). At this point, centrifugal pumping far exceeds capillary pumping and the siphon valve opens when emptying of the reservoir can be sped up by increasing the disc spin rate/centrifugal pumping force [36]. Variations of siphon valves including centrifugo-pneumatic siphon valves [45], sequential siphon valves [46,47], and interruptible siphon valves [48] can also be used for additional control.

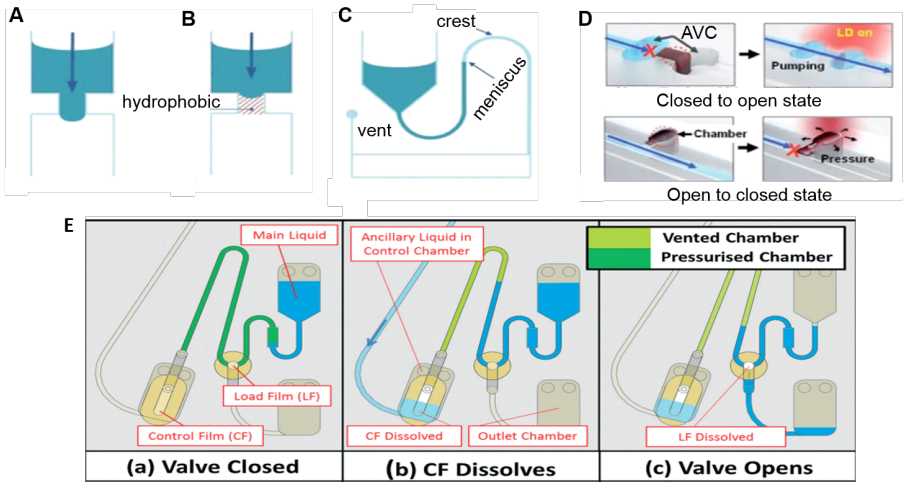

Figure 3. Centrifugal microfluidics valving methods: (**A**) capillary valve on a hydrophilic microchannel; (**B**) hydrophobic and (**C**) siphon valves. Adapted from [36] with permission from The Royal Society of Chemistry. (**D**) Laser irradiated ferrowax microvalves: at the top, from a closed to open state, the laser beam is focused at the ferrowax that melts and flows to an assistant valve chamber (AVC); at the bottom, to block an open channel, the laser is focused at the pre-loaded ferrowax located adjacent to the main channel. The molten ferrowax bursts into the main channel and solidifies, blocking it. Adapted from [49] with permission from The Royal Society of Chemistry; and (**E**) event-triggered valve based on dissolvable film (DF): (**a**) sample is loaded and the two DF tabs create a closed pneumatic chamber. The counteracting gas pressure keeps preventing the liquid to enter the pneumatic chamber; (**b**) the ancillary liquid enters and dissolves the control film (CF) and the pneumatic chamber is vented, allowing the main liquid to wet the load film (LF), and (**c**) sending liquid to the outlet chamber. Reproduced from [42] with permission from The Royal Society of Chemistry.

Sacrificial valves are another common valving technology. These valves involve the integration of some material which acts as a destructible barrier layer to allow liquid release. The release can be triggered externally, for example, by laser irradiation [49] (shown in Figure 3D). Laser irradiated ferrowax (iron oxide nanoparticles dispersed in paraffin) microvalves goes from a closed to open state by laser irradiating the ferrowax, which melts and flows to an assistant valve chamber (AVC). From open to closed state, the laser is focused at the pre-loaded ferrowax located adjacent to the main channel. The molten ferrowax bursts into the main channel and solidifies, blocking it [49]. Dissolvable films (DFs)-based valves [50–52] allow the passage of the fluid when its surface is wet, and can be used to implement an event-triggered system (Figure 3E) [42] which act analagous to a (single-use) electrical relay or transistor. DF valves are schematically positioned at specific sites on the disc, the arrival of liquid at this point triggers the release of liquid at another point [42]. In Figure 3E, the sample (main liquid) is loaded and the two DF tabs (named control film (CF) and load film (LF)) create a closed pneumatic chamber (dark green in (a)). The counteracting gas pressure keeps preventing the liquid to enter the pneumatic chamber, and thus wet the DF. At an appropriate timing, an ancillary liquid enters the control chamber and dissolves the CF, thus venting the pneumatic chamber (b), allowing the main liquid to wet the LF and finally, sending the liquid to the outlet chamber (c). This is particularly useful for sequential delivery steps when the arriving of a liquid in the waste chamber triggers the delivery of the next reagent/buffer. Many novel valving strategies have been described in the literature in the last years, always aiming to facilitate and automate disc protocols, as new passive [53–55] and active (magnetically induced [56], pinch-based valves [57], reversible [58–61], among others) valves. Some of them will be discussed in the next sections as they appear in the control of biosensors processes.

3. LoaD Fabrication

3.1. Polymer Microfabrication

At the end of the 1990s decade, polymers started to be used for microfabrication [62,63]. Opposite to silicon and glass, which are fragile and expensive, requiring time-consuming and complex processing, polymers are low-cost, of easy and scalable processing, and are available with a range of chemical and physical properties. LoaD fabrication techniques have followed the same strategies than conventional polymer-based chips. The choice of the material accounts on the cost, but especially on the desired properties, e.g., on-disc colorimetric measurement demands optically transparent polymers, some types of valves demands flexible structures, intricate design demands polymers which can be processed by high resolution techniques. As many specialised reviews have dedicated on microfabrication techniques [64–66], this review does not intend to go deep in such subject but displays the main LoaD fabrication approaches and offer the address to find out more about it.

A LoaD biosensor shelters various LUOs and commonly a net of 3D channels and reservoirs are needed, which is obtained by stacking of independently processed layers bonded to each other. The LoaD architecture is created in a computer-aided design (CAD) software, and each layer is previously processed by techniques as replica moulding (soft-lithography), xurography, laser ablation, etc. Figure 4A illustrate (a) 1.5 mm thick-poly(methyl methacrylate) (PMMA) plates machined using a CO_2 laser ablation, and (b) 86 µm thick-pressure sensitive adhesive (PSA) processed by a knife-cutter. (c) After removing the protective covers, the LoaD is assembled by stacking the PMMA and PSA layers using an alignment jig and were rolled using a laminating machine. The side view is shown in (d). Although the cutting process is automated and scalable, the assembly stage is more difficult to be automated while the manual assembly of layers is time-consuming and laborious. Yet, researchers widely use this approach at the proof-of-concept stage because the prototyping is fast and without the need for mould fabrication.

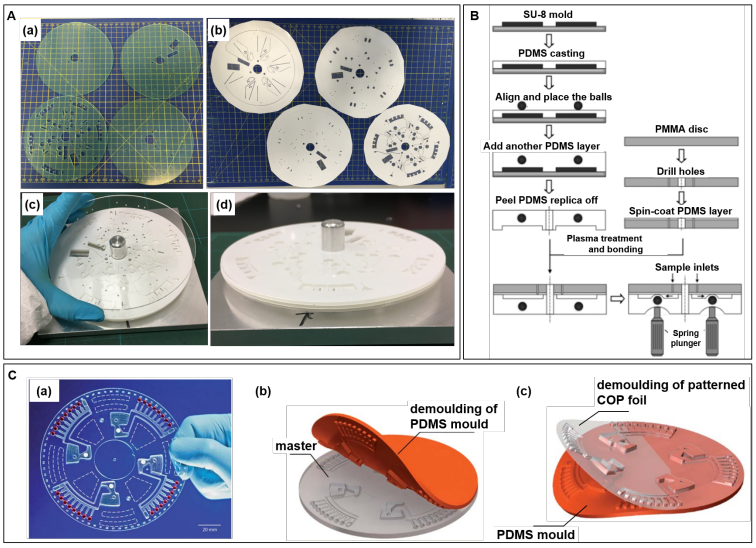

Figure 4. (**A**) Photographs of steps of layers assembly during the LoaD manufacture: (**a**) laser ablation cut PMMA discs, (**b**) knife-cut PSA layers, (**c**) stacking and alignment of layers, and (**d**) side view during the mounting of layers. (**B**) Schematics of PDMS moulding to fabricate the disc: Pinch valves-based disc fabricated by PDMS moulding. Reproduced from [57] with permission from Elsevier. (**C**) Hot embossing fabricated LoaD biosensor: (**a**) photograph of the LoaD, (**b**) fabrication of the PDMS mold using a milled PMMA master, and (**c**) demoulding of the hot embossed COP foil. Reproduced from [67] with permission from The Royal Society of Chemistry.

Polydimethylsiloxane (PDMS) is usually patterned by replica moulding (soft-lithography) in which the PDMS reagents (base + curing agent) is poured over the master mould and cured to solidify.

Commonly, the master mould is fabricated using UV photolithography of SU-8 (negative photoresist) exposing the pattern through a mask. The unexposed parts are dissolved while the cured photoresist remains on the substrate defining the pattern. Figure 4B illustrates a schematics of fabrication of a microfluidic disc by PDMS casting over the SU-8 master mould. At the design suggested by the authors to create pinch-valves, metal balls were placed over the first cured PDMS layer, and covered with a new layer of PDMS. The PDMS replica containing the metal balls are peeled off and united to a PDMS-coated and plasma-treated PMMA disc [57]. The active valves are controlled by spring plungers which push the balls deforming the flexible PDMS to block the flow [57]. Alternative low-cost techniques for master fabrication, as micromilling, laser engraving, cutting plotters, are discussed in [66]. PDMS is optically transparent in the visible range, biocompatible, flexible, and can be easily sealed to glass or another PDMS part (no need of adhesive layers). Soft-lithography provides high-resolution replicas (nm-scale), but pattern deformations and defects in the moulded product can occur in the peeling process [64]. Other disadvantages concern the cost, relatively high when compared to common thermoplastics [65], and the difficult to implement mass production [66]. Details in PDMS micromolding can be found in [68,69].

Hot embossing and injection moulding of thermoplastic materials are remarkable concerning cost-efficient mass production [70–72]. At hot embossing processing, the temperature is elevated above the polymer glass transition temperature (T_g), and the mould is pressed against the polymer substrate transferring the pattern [73]. Nanometre range can be achieved by hot embossing [71]. As polymer pattern resolution depends on the mould resolution, delicate patterns usually demand lithography/etching processed silicon moulds [70,74] accompanied by time-consuming and expensive fabrication [64]. In addition, the masters have limited cycles of life due to cracking and warping from the stress and temperature conditions [75]. To overcome these drawbacks, µ-scale PDMS patterns were produced by photolithography to act as hot embossing mould [75,76]. PDMS moulds are relatively inexpensive, rapid to fabricate and reusable for many replications, and possess thermal stability that enables to stamp common thermoplastic polymers [75,76]. Figure 4C present (a) a photograph of a cyclic olefin polymer (COP) foil disk, fabricated by hot embossing and sealed with PSA, and representations of (b) demoulding of the PDMS mould from the milled PMMA master, and (c) demoulding of patterned COP foil after hot embossing, cooling, venting, and opening of the chamber [67].

3D printing is an emerging technology in microfluidics [77]. Yet, it has some limitations concerning resolution. Usually, supporting material is needed to fill the void spaces during the printing process. Later, its removal is manually made which is time-consuming and difficult to do in small channels. The solvent assisted removing is mostly hampered because the chemical composition of supporting and construction materials are often similar [78]. The produced rough surfaces may also cause dead volumes and irregular surface modifications [78]. Concerning LoaD applications, 3D printing has been used to fabricated specific parts, as valves [61] or valve actuating discs [57,59], or in the manufacture of peripheral structures [25].

3.2. Immobilisation of the Biorecognition Element

The immobilisation of the biorecognition element is always a concern in the construction of biosensors because the sensitivity depends on the total activity of proteins. LoaD platforms, like most microfluidic devices, are usually built in polymer materials, and the direct passive adsorption of proteins as antibodies and enzymes onto these surfaces is mainly driven by hydrophobic interactions. The adsorption-induced conformation changes can lead to protein denaturation and reduce protein activity by as much as 90% [79,80]. Since hydrophobic surfaces induces higher denaturation than hydrophilic ones [81], some surface modification strategies have been proposed to increase the hydrophilicity of conventional polymers for microfabrication. These strategies include plasma treatment [82], coverage with layers of hydrophilic polymers [83,84] and graphene oxide [85]. Poly(ethyleneimine)—PEI introduces hydrophilic amine groups and acts as a spacer

(increases the space between the biomolecules and the hydrophobic surface) and has been applied in PMMA [80,84,85] and cycloolefin [83] surfaces. PEI coating [80], PEI coating following oxygen plasma treatment [84], and nanostructured layer-by-layer film of PEI and graphene oxide [85] have all demonstrated capacity to improve ELISA performance on PMMA surfaces. Functionalisation of metal surfaces is also crucial for electrochemical and reflectivity-based approaches. Conventional methods based on thiol functionalisation using cysteamine and alkanethiols followed by NHS-EDC chemistry have also been applied to the LoaD [86,87].

The anchoring of bio-active beads within the LoaD to act for the biorecognition element anchoring is an alternative to direct immobilisation of biomarkers onto the flat polymer surface. Beads can be easily functionalised with the biorecognition element *a priori* off-chip and then be loaded to the microfluidic platform. This is particularly useful when the protein coating may cause difficulty sealing microfluidic chips when surfaces have been functionalised [88]. One of the most important advantages using beads is the higher surface to volume ratio (1 g of microbeads with a 0.1 µm-diameter has a surface area of 60 m^2) [89]. This can be achieved, for example, by a 3D column filled by the functionalised beads. Additionally, analytes and bioreagents can be easily transported in the fluidic system when attached to beads, by the centrifugal flow or by external forces as pressure-driven flow or especially, by the magnetic force [89,90]. Additionally, some protein-functionalised beads are commercially available or have well-established protein anchoring protocols. Immunoassays applications usually encompass the capture antibody anchoring via carbodiimide chemistry on carboxylated-beads [91,92], or by biotinylated antibodies on streptavidin-coated particles [93].

4. Essential Processes in LoaD Biosensing

4.1. Reagents and Sample Storage and Supply

At the R & D stage, the input of reagents in a LoaD platform is usually by manual loading, via pipetting, of the reagents and samples. However, long-term storage strategies, which minimises operator handling, reduces cold-chain requirements, reduces the need for specialised user-training, and which avoids contamination of both user and sample, are of critical importance. A number of different technologies have been demonstrated including stick-packages [94,95], glass ampoules [96], and elastic-membrane micro-dispensers [97].

Pre-storage of reagents in glass ampoules placed on LoaD platforms for DNA extraction was demonstrated with no loss of ethanol and water for 300 days at room temperature. Frozen storage was also possible without ampoule rupture. The release of liquids (buffers and ethanol) is made by a mechanical force (fingertip pressure) through the elastic lid of the cartridge. While the liquid is centrifugally displaced, a filter prevents the glass shivers to go forward [96]. van Oordt et al. [94] have developed stick-packs of aluminium/polyethylene composite foil aiming at long-term storage of reagents. The transverse frangible seal was fabricated by ultrasonic welding and it is adjustable for a specific burst pressure. The hermetically sealed stick-packs can store both liquid or dry reagents, with the first frangible seal (that separates solid and liquid) bursting at lower rotation frequency. After mixing, the second frangible seal bursts to release the mixture [94]. These stick-packs were further applied in a LoaD for nucleic acid-based detection of respiratory pathogens [95].

A long-term storage micro-dispenser was created by Kazemzadeh et al. [97] and tested in lab-on-a-chip and LoaD platforms. The micro-dispenser comprises a tube with a hole and an elastic membrane covering this hole. When the internal pressure is increased (by the centrifugal force) in enough amount to stretch the membrane, a path is provided for the liquid release. Figure 5A(a) illustrates the micro-dispenser placed on a disc. No liquid release happens while the centrifugal force does not exceed the membrane force. Increasing the internal pressure by the rotation speed, membrane stretches and releases the fluid (b). To implement this technology for blood separation, a micro-dispenser was created with a tube with two apertures, each one covered with different elastic materials (see Figure 5B(a)). The top and the bottom membranes are for plasma and blood cells delivery,

respectively. The location of each aperture is well-planned, e.g., the first top aperture is located at a point above the level where the plasma is separated from blood cells. Figure 5B(b) illustrates three identical assays for blood separation on disc and (c) a single assay with a micro-dispenser placed on the disc with a piece of tape and a tacky adhesive. Because of the different elastic properties, each of the membranes releases the liquid at different rotation speeds. In this case, a higher centrifugal force is needed to release the blood cells (bottom membrane). The long-term stability of the micro-dispensers were demonstrated to be two and one year(s), for DI-water and ethanol 70%, respectively [97].

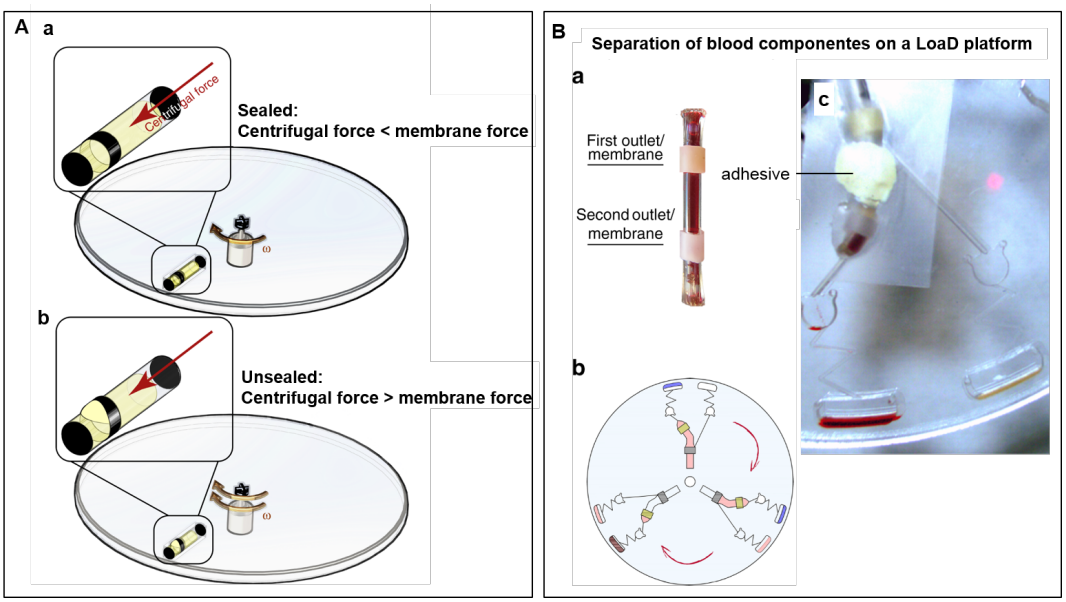

Figure 5. (**A**) Micro-dispenser working principle in a LoaD platform. (**a**) When the centrifugal force is lower than the membrane resistance, no liquid is released. (**b**) Increasing the rotation speed, the centrifugal force overcomes the membrane force and the fluid is temporary released. (**B**) Separation of blood on a LoaD platform. (**a**) Micro-dispenser with two apertures covered with two different membranes, C-flex and latex, and (**b**) a schematic of the LoaD platform for 3 identical assays for blood separation. (**c**) Picture of the disc dispensing blood plasma and blood cells to two different chambers at different rotation frequencies due to the difference in the membranes properties. Reproduced from [97] under a Creative Commons Attribution 4.0 International License.

4.2. Samples and Reagents Processing

4.2.1. Blood Processing

Blood is the most utilised sample for diagnostics, and its separation is usually the first step of many biological assays. Cell isolation and pathogens detection demand an initial step of selective blood separation. Conventional benchtop processes typically use centrifugation. This is relatively simple but often requires large sample volumes and, in case of infectious disease, there are concerns about operator safety. Based on the different densities of blood components, it is quite easy to promote separations simply by the rotation of the disc. Common protocols for plasma extraction on disc use moderate (about 1200 RPM for 3–8 min [98,99]) to fast rotation (2000–5000 RPM for few seconds [100–103]). Due to the difference in density of the plasma and the red and white blood cells, blood cells are driven toward the bottom while the plasma forms the supernatant layer on the top [101]. One of the great advantages of LoaD platforms is that the plasma extraction step can be easily and conveniently integrated with the following metering, mixing, and detection steps. It has been reported for plasma extraction, metering and mixing with reagents for the prothrombin (PT) time tests [101–103], nitrate/nitrite assays [98], cancer cells detection [86,104], virus detection [90] and many other sensing platforms.

Some geometry parameters can be defined to increase the speed of blood separation. Kim et al. [105] found that higher tilt angles and narrower channels promote faster plasma separation. The enhanced sedimentation in inclined channels is known as Boycott effect [106], and it is associated with the increase in the surface area available for the particles settling [105]. The impact of the Coriolis force on blood sedimentation has also been investigated [107]. *Spira mirabilis*-like structures (equiangular spiral) demonstrated an enhanced speed of sedimentation due to the increased Boycott effect, herein applied with a density gradient medium (DGM) [108]. Sedimentation over DGM uses solutions with specific densities, such as Ficoll and Percoll, to separate and sort blood cells into layers according to their inherent density differences [109]. This can facilitate the collection of the separated components, and thus the analysis of multiple blood samples. Figure 6A(a) illustrates the density distribution of human blood cells and (b) a schematic of the separation using Ficoll (density = 1.077 g mL^{-1}), with the dense cells moving to the bottom while the low density-cells remain on the top layer. Efforts have been done to develop DGM-based blood fractionation and separation of specific cells [21,86,104,110–113]. Morijiri et al. [113] proposed an elutriation-based separation in a centrifugal disc. Particles are introduced in the separation chamber with a low-density fluid under centrifugation. While particles experienced a centrifugal force in an outward direction, the fluid force acts in an inward direction. The retention position of each particle depends on the size and density, and are controlled by the balance of the centrifugal force and the fluid drag force. Small and low-density particles are not retained in the separation chamber and are the first to move towards the outlet. By introducing solutions with higher densities, the balance of forces is changed allowing a step-wise elution and recovery of particles [113].

Leukocytes extraction can be particularly important. Abnormal leukocytes counts can be related to anemia, infection, inflammatory conditions, and certain cancers [114]. Furthermore, they can interfere with the detection of circulating tumor cells (CTCs) [104]. CTCs have large size variation and their size can overlap with leukocytes causing unreliable size-based separations. Because CTCs are disseminated from primary tumors or metastatic sites to the bloodstream, LoaD platforms to separate them from whole blood have been developed [115,116]. Park et al. [104] developed a centrifugal platform with the selectivity based on the anti-EpCAM covered microbeads, which specifically bind to the CTCs, and thus make them heavier than other blood cells. This leads to sedimentation through a DGM and thus being isolated. Figure 6B shows the disc designed for sorting CTCs (left). The blood sample and microbeads conjugated with anti-EpCAM were injected via the blood chamber inlet while the DGM (Percoll) was pipetted through the DGM chamber inlet. Blood and microbeads are shown in the blood chamber (a), and after plasma separation, the triangle obstacle structure (TOS) played a role to retard the convection of the separated blood cells in the blood cell zone while the disc is stopped to open valve 1—V1 (to remove plasma to the waste chamber) (b). After the complete removal of plasma (c), V2 is closed to initiate the bead-binding (incubation) process by mixing (d). V3 is opened and the sample was transferred to the DGM chamber, where under centrifugation the microbeads-CTCs complexes were moved to the collection chamber, passing through the DGM layer due to their higher density, while the other cells remain on the top (e). After the complete separation, V4 is closed before the collection to avoid contamination (f) [104]. Here, the valving was based on the laser irradiation ferrowax [49], discussed previously.

Filtration-based strategies have also been successfully applied for blood separation. Sequential and tangential flow filtration using two track-etched polycarbonate membranes were integrated in the chambers by Kim et al. [117]. The pore size of the filters was carefully selected considering the size of platelets and blood cells. Figure 6C(a) depicts a photograph of the platelet isolation disc highlighting the filters. Schematics in Figure 6C(b) shows Filter-I (3 µm) to eliminate both white blood cells (8–15 µm) and red blood cells (6–8 µm). The plasma runs through Filter-II (600 nm) which captures platelets while washing residual plasma contents out to the waste chamber, as extracellular vesicles, proteins, lipids, and cell-free DNA [117]. Platelet analysis revealed high purity (>99%), free of white blood cells contamination, and the yield of the platelets recovery was significantly superior (>fourfold)

than that conventional benchtop centrifugation [117]. Refer to the source for more details [117]. Table 1 summarises the blood separation and analysis integrated into LoaD platforms.

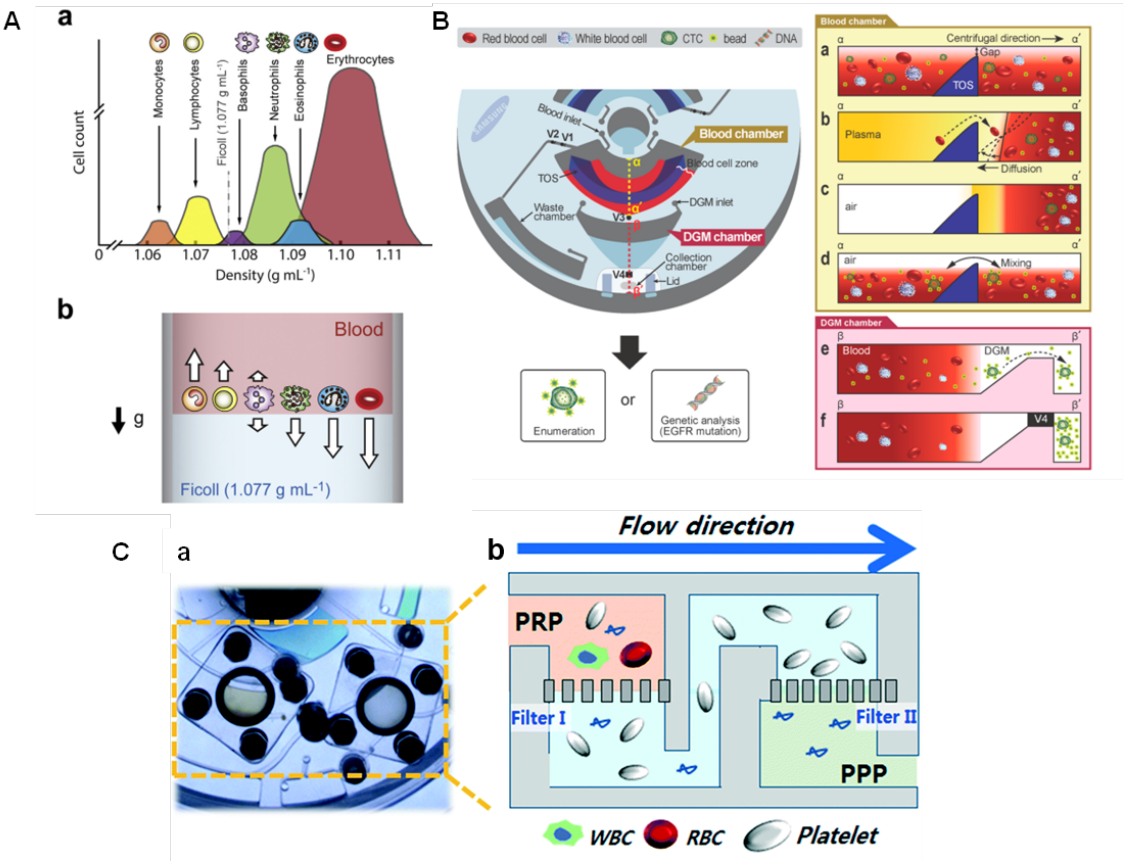

Figure 6. (**A**) Sorting of blood cells based on the DGM centrifugation. (**a**) The density distribution of human blood cells and (**b**) the movement of blood cells upon centrifugation with blood layer placed on the top of the Ficoll solution. The arrows indicate the movement direction of cells. Reproduced from [109] with permission from Elsevier. (**B**) Disc design for sorting CTCs from whole blood. TOS: triangle obstacle structure; V1, V2, V3, and V4 are on/off operation valves (wax that changes from liquid to solid state) controlled by laser irradiation. (**a**) Cross-sectional view of the blood chamber after injection of blood and microbeads; (**b**) after plasma separation; (**c**) after removal of the plasma with opening V1; (**d**) during incubation to bind CTCs to the antibody-functionalised beads; (**e**) the cross-sectional view of the DGM chamber showing that only CTC-microbead complexes (with higher density than DGM) are moved to the collection chamber; (**f**) V4 is closed to prevent sample contamination during collection. Reprinted with permission from [104]. Copyright 2014 American Chemical Society. (**C**) Filtration-based platelet isolation disc: (**a**) photograph and (**b**) schematics. Filter-I to eliminate both white blood cells and red blood cells from a platelet-rich-plasma (PRP). PRP runs through Filter-II which captures platelets while washing platelet-poor plasma (PPP) out to the waste chamber. Reproduced from [117] with permission from The Royal Society of Chemistry.

Table 1. Summary of the blood separation strategies performed in LoaD platforms. WB: whole blood, DGM: density gradient medium, PT: prothrombin time, HBV: hepatitis B virus, PBMC: peripheral blood mononuclear cell, CTC: circulating tumour cells, CRP: C-reactive protein, IL-6: interleukin-6.

Ref	Portion of Interest	WB Volume (Extracted Volume)	Separation Protocol	Separation Approach	Achievement
[98]	Plasma	70 µL (10 µL)	3 min @ 1200 RPM	Simple centrifugation	Successfully applied to nitrate and nitrite detection
[100]	Plasma	1 µL	1.5–6.0 s @ 1800 RPM	Simple centrifugation	Plasma separation efficiency of 96 %
[101]	Plasma	2.0 µL (0.5 µL)	2.5 min @ 2200 RPM	Simple centrifugation	Successfully applied to PT test.
[102]	Plasma	14 µL (3 µL)	80 s @ 4000 RPM	Simple centrifugation	Successfully applied to PT test
[103]	Plasma	7 µL (2 µL)	90 s @ 5000 RPM	Simple centrifugation	Successfully applied to PT test
[86]	Cells	5 assays × 20 µL	5 min @ 1500 RPM	DGM based separation and antibody functionalised sensor	Cell capture efficiency of 87% and CTC detection via EIS
[104]	Cells	5 mL	640 s @ 3000 RPM	Geometry + DGM	90% recovery of CTC isolation
[90]	Serum	500 µL (200 µL)	90 s @ 60 Hz	Simple centrifugation	Recovery of 90%. Successfully applied to PCR HBV detection
[21]	PBMC	18 µL	60 Hz	DGM	34% efficiency compared to hospital laboratory data
[110]	PBMC	8.75 µL	4 min @ 45 Hz	DGM	73% PBMC extraction (27 % below hospital laboratory data)
[111]	Cells	3 µL total (WB + beads)	40 min @ 10 Hz	centrifugo- magnetophoresis	92% efficiency of cells isolation
[112]	Blood fractions	10 µL	4 min @ 2700 RPM	Simple centrifugation with capillary valves to keep layers separated	95.15% leukocytes extraction
[113]	Blood fractions	20 µL diluted WB	720 s (+ 900 s) @ 2000 RPM (for erytrocytes elution/separation)	centrifugo- elutriation (balance between centrifugal force and fluid drag force)	98% recovery of erytrocytes
[117]	Plasma (platelet purification)	600 µL (150 µL platelet sample)	5 min @ 3000 RPM	Filtration-based isolation	99% purity with total assay time including washing = 20 min
[118]	Protein isolation	1 µL	5 min @ 8000–9000 RPM	DGM and antibody functionalised beads	CRP and IL-6 quantification (total assay time of 15 min)

4.2.2. Volume Metering and Aliquoting

Accurate metering of reagents and samples is an essential step in sample preparation to guarantee a reproducible and quantitatively reliable response from the biosensor. Although different architectures are found in the literature, the volume metering in LoaD is based on the chamber volume (controlled by its geometric parameters). Typically, an overflow channel is connected to this metering chamber to guarantee that any excess of liquid is sent to a waste/overflow chamber, as illustrated in Figure 7A. The same overflow principle can be applied to implement aliquoting and serial dilutions on disc, which are usually time-consuming and susceptible to errors (specially when working in µL-scale) when performed manually. As depicted in Figure 7B, Mark et al. [119] developed a metering structure whereby a dead-end pneumatic chamber enhanced system performance. In this structure, a single metering chamber is connected upstream and downstream by a feeding/overflow channel. The volume metering is based on centrifugo-pneumatic valve structure in which the metering chamber V_M is connected by a narrow channel to an unvented receiving chamber V_0 (a). The volume metering chamber is filled but the receiving chamber, which may, for example, contain lyophilised reagents, remains dry (b). When liquid reaches the narrow connection at the bottom, a meniscus is formed which prevents the air from escaping the unvented receiving chamber (creates a pressurised chamber with pressure p_1) (c). Aliquoting is performed by continuing the liquid feed. After complete the first V_M (d), the overflow channel deliveries the liquid for the next metering channel and so on, as illustrated in Figure 7C(a). After all the metering channels are completed, an increase in the centrifugal frequency reaches a point (burst frequency) in which the centrifugal force overcomes p_1, releasing the liquid to the receiving chambers, as shown in Figure 7B(e),C(b).

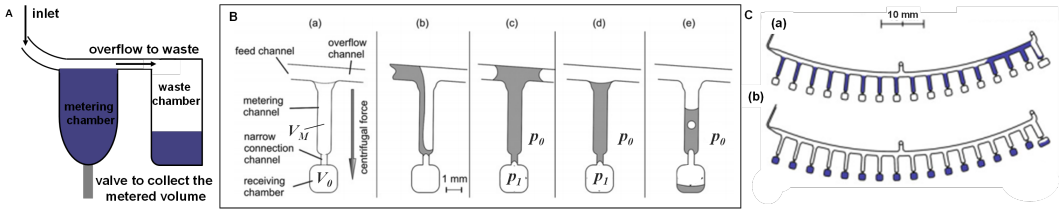

Figure 7. (**A**) Simple metering design based on overflow. (**B**) Metering structure based on the centrifugo-pneumatic valve: (**a**) design of a single metering structure with the volume defined by the metering channel V_M. (**b**) At a first centrifugal frequency, liquid fills the metering channel while air is displaced. (**c**) The pressure p_1 prevents the liquid to enter the receiving chamber V_0. (**d**) After metering, (**e**) an increase in the centrifugal frequency above the burst frequency (to an amount that overcomes p_1) releases the liquid. Adapted from [120] with permission from The Royal Society of Chemistry. (**C**) Layout of an aliquoting structure: (**a**) multiple V_M chambers been fed by liquid, and (**b**) aliquots distributed to the receiving chambers. Adapted by permission from Springer Nature [119], Copyright 2011.

Active valving based on individually addressable diaphragm (ID) valves [61] was used for on-disc serial dilutions by Kim et al. [121] (Figure 8A). These valves are assembled from an elastic epoxy diaphragm and a 3D printed actuator (Figure 8B). A simple push-and-twist action is required for closing and opening the channel. This open/close functionality allows the volume of sample and buffer to be metered in the two different zones; thus dictating the degree of dilution. These two zones are detailed in Figure 8C,D. An example of fivefold dilution is presented in Figure 8E (opened and closed valves represented by green and red colours, respectively): (i) at buffer metering zone, valve 1 (V1) is opened while V2, V3, V4, and V5 are closed for metering of total 9 µL-buffer. Simultaneously, at the sample metering zone, V6 and V7 are opened while V8 is closed, totaling 8 µL sample metered; (ii) at the sample metering zone, V6 is closed and the 8 µL-metered sample is sent to R1 (with valves 7, 8, 9, and 10 opened while V11 is closed). From the initial 10 µL sample, 2 µL remains in the mixing chamber. At the buffer metering zone, only the V5 is kept open, sending the buffer excess to the waste chamber; (iii) the 2 µL sample in the mixing chamber is diluted by the delivery of 8 µL buffer

(only V2 and V3 are opened while V4 is kept closed keeping 1 µL buffer retained). Finally, the 5-fold diluted solution is metered (5 µL, by keeping V6 opened while V7 is closed) and sent to R2. The next dilution can be performed to the remained solution in the mixing chamber based on the similar steps (protocols for 2-,5-, and 10-fold dilutions are summarised in the table of Figure 8E). Buffer can be re-loaded by opening V1 [121]. Although the system at first appears complex and unwieldy, the recent miniaturisation and cost-reduction in micro-controllers means this approach can be easily automated and can flexibly address a wide array of biosensor applications.

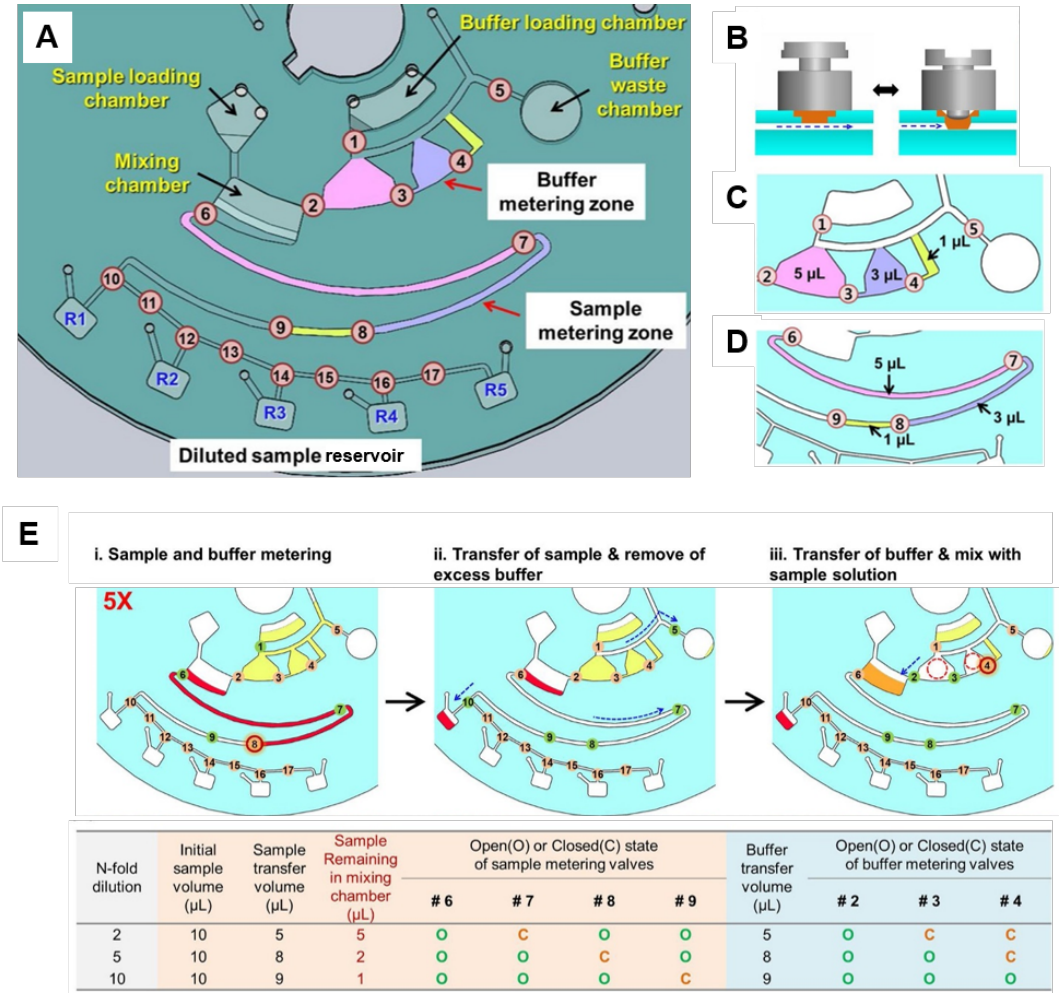

N-fold dilution	Initial sample volume (µL)	Sample transfer volume (µL)	Sample Remaining in mixing chamber (µL)	Open(O) or Closed(C) state of sample metering valves				Buffer transfer volume (µL)	Open(O) or Closed(C) state of buffer metering valves		
				# 6	# 7	# 8	# 9		# 2	# 3	# 4
2	10	5	5	O	C	O	O	5	O	C	C
5	10	8	2	O	O	C	O	8	O	O	C
10	10	9	1	O	O	O	C	9	O	O	O

Figure 8. (**A**) Disc design for serial dilution consisting of sample and buffer loading chambers, mixing chamber and buffer waste chamber, two metering zones (for sample and buffer), five collecting reservoirs (R1–R5) for the diluted samples and seventeen ID valves (numbered circles). (**B**) A reversible ID valve composed of a diaphragm (orange) embedded on a top layer and 3D printed valve actuator (gray). Simple push and twist actions open and close the channel. Detailed buffer (**C**) and sample (**D**) metering zones. (**E**) 5-fold dilution steps: (i) in the buffer metering zone, a total of 9 µL is metered keeping V1 opened while V2, V3, V4, and V5 are closed. At the sample metering zone, V6 and V7 are opened while V8 is closed, totaling 8 µL metered; (ii) at the sample metering zone, V6 is closed and the metered liquid within the channel is sent to R1 (V7, V8, V9, and V10 are open while V11 is closed). At the buffer metering zone, V1, V2, V3, and V4 are closed and V5 is opened to send the excess to the waste chamber; (iii) 8 µL buffer is delivered (just V2 and V3 are open while V4 is kept closed keeping 1 µL of buffer retained) into the mixing chamber, where remains 2 µL sample. Thus, a dilution of 2 µL sample to a final 10 µL volume solution was achieved. The table presents the summary of the metered volume of sample and buffer, and the state of the valves to achieve 2-, 5-, and 10-fold dilutions. Reproduced from [121] with permission from Elsevier.

4.3. Mixing and Washing

Mixing protocols should provide an effective and fast homogenisation of the fluids. However, adaptation of simple bench-top protocols as agitation, vortexing and stirring onto the LoaD can cause unwanted opening of rotationally actuated valves; and the subsequent uncontrolled pumping of liquid. Therefore, systems which require rigorous mixing must be carefully designed. Several studies have been focused on developing disc protocols to allow an integrated and adequate mixing. On-disc mixing can be passive, just based on the rotation control, based on intrinsic forces as Euler or Coriolis [122–124] or by means of control of geometry [125,126]; or can be active based on external perturbations, e.g., compression by external actuators [127] or use of magnetic-beads inside the disc in combination with permanent magnets [128,129]. Several micromixing technologies are discussed in [130].

One of the most utilised mixing protocol is the "shake-mode" mixing [124] comprising periodic changes in the sense of rotation and rapid changes of the spinning frequency. The difference in the angular momentum leads to the appearance of a shear force that drives an advective current within the liquid [124]. The mixing time was down to 3.0 s for 25 µL-volume while a mere diffusion-based mixing took about 7 min. Combining the "shake-mode" mixing with magnetic beads (pre-filled in the mixing chamber) periodically deflected by a set of permanent magnets resting in the lab-frame, an effective homogenisation was attained in only 0.5 s [124].

The use of pneumatic pressure to promote reciprocating flow-based mixing [131] was introduced later, and has been successfully applied in LoaD biosensors [87,132]. This scheme utilises an auxiliary pneumatic chamber, and the sequential decrease and increase in the centrifugal force causes the compression and decompression of air pushing the liquid through different chambers and thus allowing an accelerate mixing [131]. Figure 9A(a) depicts an immunoassay disc. The biorecognition element (antigen) is immobilised on the reaction chamber to specifically capture the primary antibody (sample) while the secondary antibody is to allow the colorimetric detection. The schematics is illustrated in Figure 9B(b). The sequence of images in (c) describes: (i) the sample stored in the loading chamber; (ii) acceleration causing air compression in the pressure chamber; (iii) by deceleration, the air expansion in the pressurised chamber pushes the liquid back to the upper chamber; (ii and iii) the increase and decrease in rotation speed (3200–7000 RPM) are reciprocated to effective and rapid mixing; (iv) the rotation frequency is increased to the maximum (7500 RPM); followed by (v) a rapid decrease to very low value (480 RPM). This increases the liquid level above the crest point, primes the siphon valve and sends liquid to the waste chamber, (vi) leaving an empty reaction chamber [132]. Pneumatic valving and mixing are reviewed in [133]. Another reciprocating mixing technology demands lower rotation frequency (0–1500 RPM) and encompass the micro-balloon pumping [134]. With higher centrifugal force, the liquid is pushed into an air chamber inflating a latex micro-balloon. A reciprocating mixing can be performed increasing (inflating the micro-balloon) and decreasing (flattening the micro-balloon) the rotation frequency [134].

Additionally, mixing can be done with gas bubbles integrating external pumps [135] or with gas generation by internal reactions [136]. Figure 9B illustrates the schematics and images from two separated layers of solutions contained in a vented reservoir (top channel) (a), air pushing through the lower channel creates bubbles that promote the mixing (b), thus creating a homogeneous solution in about 100 ms (c) [135]. To avoid the need of external apparatus, Burger et al. [136] implemented a bubble-based mixing by gas produced through a chemical reaction (Figure 9C(a)). The oxygen bubbles are generated in the reaction chamber by the hydrogen peroxide decomposition, which provokes a drag flow through the liquid. A strong buoyancy causes deformation and rupture of these bubbles inducing mixing flows, as represented in (b). In a DNA extraction experiment, this approach allowed a similar performance compared to the "shake-mode" mixing and can be an alternative approach when mixing has to be performed at a fixed rotational frequency.

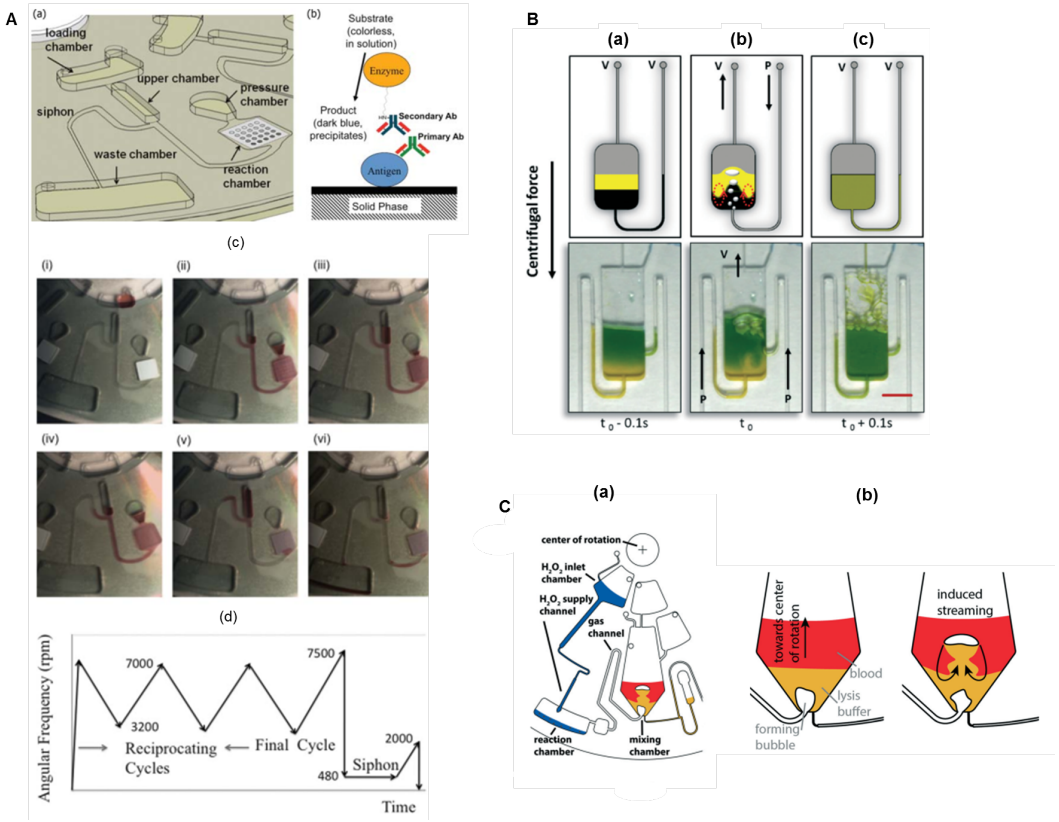

Figure 9. (**A**) Pneumatic pressure flow-based reciprocating mixing. Schematics of (**a**) the fluidic system and (**b**) the antibody capture assay to take place in the reaction chamber; (**c**) images of the system in operation: (i) sample is loaded; (ii) the increase in the rotation frequency promotes the air compression in the pressure chamber; (iii) the decrease in the rotation speed promotes the air expansion that pumps the liquid towards the center; (ii) and (iii) can be repeated in a reciprocated manner. (iv) The increase of rotation to the highest speed (7500 RPM) followed by (v) a decrease to the lowest rotation frequency (480 RPM, see protocol in (**d**)) allow the liquid to prime the siphon valve and (vi) send the liquid to the waste chamber. Reprinted from [132], with permission of AIP Publishing. (**B**) Bubble-based mixing schematics with an external pump: (**a**) from an unmixed state of two dyes, (**b**) under bubbling mixing, to (**c**) a homogeneous solution. Reproduced from [135] with permission from The Royal Society of Chemistry. (**C**) Buoyancy driven bubble mixer set-up. (**a**) Hydrogen peroxide flows into the reaction chamber and the decomposition reaction produces oxygen which is directed through the gas channel to the mixing chamber. (**b**) The mixing chamber with blood and lysis buffer in separated layers (left) and a bubble detaching and ascending through the liquid (right). Reproduced from [136] with permission from The Royal Society of Chemistry.

Mixing and washing steps are crucial for biosensors concerning especially the incubation of the sample with the biorecognition element, which is fundamental for biochemical reactions to occur. Incubation can be performed at a constant low rotation for some assays (400–600 RPM for few minutes [98,137]), while longer periods are necessary for some complex assays such as nucleic acid amplification, e.g., LAMP assays (about 60 min at low or paused rotation [138–141]), NASBA (about 70 min [142]), and RPA (about 15–30 min [143,144]). In ELISA the incubation protocols have been performed even in constant spinning (at 20 Hz for 15 min [85]) or in mixing modes ("shake-mode" mixing from 15 to 30 Hz for 10 min [99] or by magneto-balloon assisted mixing at 900 RPM for 30 min [60]). Incubation protocols should be developed and optimised individually for an assay. In biosensors based on the formation of a complex of magnetic nanoclusters with antibody- [145] or aptamer- [146], the presence of the target triggers the magnetic particles agglutination, which is quantified with an optomagnetic readout. A two-step protocol promoted reliable results with reduced

incubation time: the first 1 s incubation step occurs in a strong magnetic field to facilitate clusters formation, followed by the second step of 2 s mixing by shaking to break unspecific bindings and to facilitate the reorientation of the beads for the readout [145,146]. A protocol with 180 cycles of incubation and mixing was established to detect the NS1 Dengue biomarker in serum [145].

After any incubation, the washing step has to guarantee that any impurities, as well as unspecific binders are removed. Washing is usually performed in "shake-mode" mixing with proper buffer solutions, and can be performed more than once if necessary. For each LoaD platform, it is important to select the most suitable approach. "Shake-mode" mixing is the simplest way to achieve good mixing in a passive set-up (no need of external devices), but demands to vary the speed rotation for relatively high frequencies. If this is not possible, external forces (e.g., magnetic or pressure) can be introduced, or bubbles can be generated internally, however, this demands a precious disc area (additional storage reservoirs) and disc area can be quite limited since many lab protocols has to be included in a LoaD biosensor.

4.4. Detection Methodologies

A broad variety of analytical approaches have been used in LoaD biosensors. There is no rule to follow concerning which method should be or should not be used in LoaD platforms, but all of them exhibit advantages and limitations that should be considered. A complete review of detection methods for centrifugal microfluidic platforms is found in [39]. If the analyte is detectable with enough sensitivity and selectivity, the optical colorimetric strategy is the most cost-effective and easy integrated readout method. With technological advances and miniaturisation of detection systems, other approaches raise attention to PoC devices. Special attention to the label-free methods as electrochemical impedance spectroscopy (EIS) and SPR (surface plasmon resonance), which can greatly simplify immunoassays by reducing fabrication-cost and fluid handling. Table 2 lists some detection techniques used in LoaD biosensors comparing the advantages, limitations and solutions, some of them especially thought to adapt the analytical detection set-up to the LoaD platform. Following, this section discusses recent and relevant developments concerning optical and electrochemical detection.

4.4.1. Optical Detection

Optical strategies require three basic components: a light source, a photodetector, and a reaction chemistry, which is analyte concentration-dependent. Particularly to the absorption and fluorescence techniques, considering that the discs can be fabricated in transparent polymers, easy integration of the detection module is possible with the optical transducer placed as a peripheral optical device without the need of electric contacts and wires. Optical strategies for centrifugal microfluidic devices are reviewed previously in [38,39]. Especially for biosensors, optical approaches are widely used because many biological analytes absorb light in a specific wavelength or can be easily marked to do so. In addition, many commercial kits were available for quantitative determination by colorimetric and fluorimetric approaches, which greatly simplifies the R & D stages of LoaD optical biosensors.

Table 2. Detection strategies in LoaD biosensors, advantages, limitations and solutions.

Detection Method	Advantages	Limitations	Solutions
Optical: UV-vis absorbance	Easy integration to LoaD (no contact is needed). Adequate to portable and inexpensive readout device.	Limited to the intrinsic analyte property or demand labelling. Limited sensitivity for thin discs (Abs depends on the light path length).	Colorimetric reagents available for many biochemical reactions. Use of thick discs, or TIR optics to increase path length [147,148].
Fluorescence	High sensitivity. Well-established analytical protocols.	Labelling with fluorescent dyes is needed, leading to complex fluid handling (sandwich assay). Relatively complex and expensive optics sometimes lead to off-disc measurements. Polymer autofluorescence can reduce sensitivity	Availability of highly sensitive and selective fluorescent labels. The use of strobe flash as light source to fluorescence allowed measurements on rotating disc [149]. Select polymers with low autofluorescence (as PDMS) [150]
Surface plasmon resonance (SPR)	AHigh sensitivity. Label-free (simple immunoassay set-up).	Expensive equipment and difficult integration. Need Au or Ag sensing surface integrated to LoaD. Results susceptible to temperature variations.	Simplified optical set-up (but less sensitive) can be implemented to µg/mL IgG detection [87]. Grating based SPR detection uses simplified optics [151].
Electrochemical:			
Impedance spectroscopy (EIS)	Label-free (simple immunoassay set-up). Independent of sample turbidity or optical path length.	Need electrodes integrated to LoaD. Rotating should be stopped to wires connection and measurement through a potentiostat.	Screen-printed electrodes [152] and gold sputtering [86] were successfully applied to electrode integration on disc. Wireless technology based potentiostat-on-a-disc (PoaD) allows on-disc and rotating disc measurements [153].
Amperometry/Voltammetry	High sensitivity. Fast response. Independent of sample turbidity or optical path length. Adequate to portable and inexpensive readout device. Multianalyte analysis in a single assay (Voltammetry).	Analyte (or co-products) should be electroactive or suspended in electroactive species solution. Need electrodes integrated on LoaD and wires connection to measurement.	Several biochemical compounds are electroactive or produce electroactive products through enzymatic reactions. PoaD can allow on disc measurements.

The Beer–Lambert Law shows the dependence of the light absorption with the absorbing species concentration, which allows a simple approach of sample quantification. A simple set of light emitting diode (LED) with the adequate wavelength emission and a proper photodetector perpendicularly aligned to the disc plane can be used to create a compact and low-cost detection module [154]. The Lambert-Beer Law also states that the absorbance depends on the optical length. Because of that, achieving a reasonable limit of detection in thin discs can be difficult. This can be overcome with thick discs, or by increasing the light path length with an optical beam-guidance set-up based on the total internal reflection (TIR) [147,148].

Various well-established colorimetric lab protocols were successfully implemented in LoaD platforms as loop mediated isothermal amplification (LAMP) and polymerase chain reaction (PCR) as well as the immunoreactions-based fluorescence-linked immuno-sorbent assay (FLISA) and enzyme-linked immuno-sorbent assay (ELISA). LAMP-based LoaD platforms for bacteria [138,139,141] and virus [155–157] detection, as well as PCR for virus [90,95,158] and bacteria [137,159] detection have been published. DNA amplification is a reliable detection method and has existed for decades. The implementation of this technique on a LoaD however is a more difficult task. The LoaD proposed by Li et al. [90] is illustrated in Figure 10, a PoC apparatus for Hepatitis B Virus (HBV) detection which boasts the same diagnostic capabilities as that of a centralised laboratory test. On-board valving allows for serum separation and reagent storage which allow for a fully automated test. A laser diode activates the valves allow for the release of reagents. Centrifugal forces generated by the double rotation axis of the microfluidic platform, which rotate to allow the stationary magnets to displace the internal capture magnetic beads for nucleic extraction. The complex system includes three resistors and thermistors which control the specific temperatures required for the PCR process. Finally, a 470 nm-blue LED served as an excitation source. The fluorescent signal was then detected using two optic fibers when the turntable containing the LoaD was position to the fixed detection region. The only user interaction required is the insertion of 500 µL of whole blood where the systems boasts an LOD of 10^2 copies/mL in just 48 min [90].

As exemplified before, nucleic acid amplification strategies, as LAMP and PCR assays, demand controlled temperature raising. Temperature sensors and heating system can be also integrated into the LoaD platform. Technologies using hot air gun [160] and heater boards [139,155] have been proposed to control temperature profiles. Figure 11A depicts a set-up for a LAMP-based bacterial infection sensing. The heater board with embedded resistive heating elements and thermistors was connected to a printed circuit board (PCB) which allows temperature control and wireless communication with a remote computer [139].

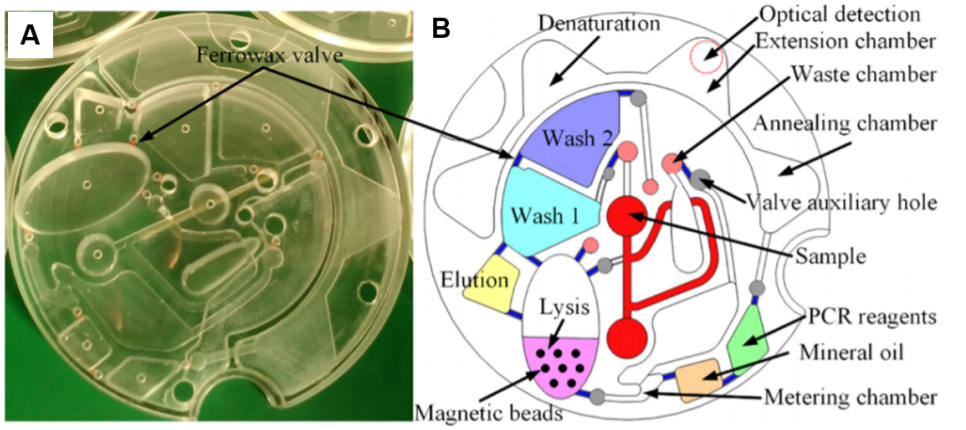

Figure 10. (**A**) The optically transparent disc and (**B**) the schematic of the LoaD architecture for HBV DNA detection in whole blood. Sample is inserted into the centre reservoir of device where pre-stored DNA extraction reagents in wash 1, 2, elution ad lysis buffers and magnetic beads. Ferrowax valves control the release and flow of each reagent to initiate the DNA extraction which then mixes with pre-stored primer and PCR reagents for amplification purposes. Reprinted with permission from [90]. Copyright 2019 American Chemical Society.

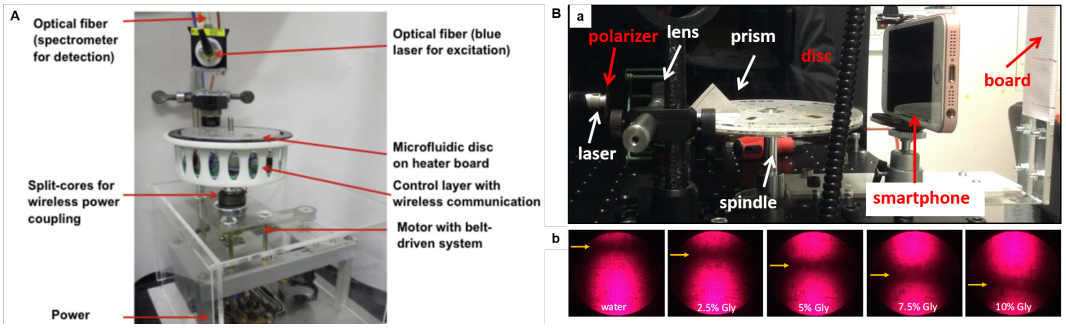

Figure 11. (**A**) LoaD set-up for LAMP assay-based bacterial infection sensor. A belt-driven motor to provide the centrifugal force; power coupling device; wireless data communication module for temperature control and signal detection; light source (blue laser at 488 nm) for the fluorescence excitation; and spectrometer linked to a data acquisition computer. The disc is on an electronic circuit board (PCB) accommodating the heating elements for microfluidic disc to the temperature control. Reproduced from [139] with permission from Elsevier. (**B**) SPR immunosensor set-up: photographs of (**a**) SPR optics integrated to a spin stand, and (**b**) the reflected laser spots from aqueous glycerol pattern solutions (with different refractive indexes) showing the position of the dark lines (caused by the plasmon absorption). Adapted from [87] with permission from Elsevier.

Immunoassays in format of ELISA [99,161] and FLISA [98,162] have also been implemented on LoaD platforms. Conventionally, the detection is made by the absorption (or emission) measurement using a monochromatic light source and an optical sensor, as demonstrated by Thiha and Ibrahim [161] with a PoC sandwich-type ELISA platform for Dengue detection. Oh et al. [163] have applied a similar colorimetric measurement, combined with LAMP, for detection of food-borne pathogens.

Immunoturbidimetry method was used to measure hemoglobin A1c (HbA1c), a glycated hemoglobin recommended by the American Diabetes Association for diabetes diagnosis [164]. The process automated on disc includes the rupture of erythrocytes by a hemolysis reagent, the attaching of the hemoglobin on latex particles, and the specific agglutination of HbA1c, which causes the solution turbidity. The specificity is given by the HbA1c monoclonal antibody added to induce the particles agglutination. A calibration curve reading the absorbance in 660 nm against Hb1Ac concentration was plotted for further quantification of hemoglobin in unknown samples. Fourteen

blood samples were tested giving a rapid response (8 min), a good correlation with laboratory results (ion-exchange chromatography), and a standard deviation of ± 0.36% HbA1c (of order with standard laboratory equipment) [164].

Despite ELISA presenting the advantage of the easy colorimetric detection, it requires labeled proteins. Label-free methods as those based on surface plasmon resonance (SPR) simplify the disc design (less reagents and washings) and reduce the production cost (labeled proteins are expensive). SPR biosensing is based on changes in the refractive index very close to the sensor surface (usually gold or silver) caused when the analyte (in solution) binds to the biorecognition element immobilised on the sensor surface [165]. Grating-based [166] and prism-based [87] SPR approaches have been proposed. We have demonstrated an SPR-LoaD platform to simple multi-analyte immunoassay adaptable to detect specific diseases just by changing the capture antibody loaded onto the gold sensor [87]. The gold sensor was attached to the top of the disc immediately before the assay running exempting the need for special storage and transport cares and generalizing the device manufacture. The SPR optics (Kretschmann configuration) were integrated to a spin stand (Figure 11B(a)), and were tested in glycerol solutions to check on the dependence of the SPR angle position with the refractive index of solution. Pictures of the reflected light spot were recorded with a smartphone camera in a dark room (shown in b), and further image analysis provided a plot of reflected light intensity versus incident angle, with the minimum reflectivity (SPR angle) caused by the plasmon absorption. Shifts in the SPR angle were proportional to the antigen concentration when the biorecognition element (specific antibody) was immobilised on the gold sensor. Details can be found in the source [87]. Although the SPR optics can appear to be complex when integrated into LoaD, automated approaches turn SPR a very sensitive optical detection technology for LoaD biosensors. The company Biosurfit (Lisbon, Portugal) already commercialises SPR-based platforms [167].

Raman [168] and surface enhanced Raman scattering (SERS) [169,170] based discs for the detection of organic compounds have been recently published bringing good perspectives for future LoaD biosensors. Because of the expensive and complex detection set-up, these methods are not appropriate to PoC devices at this point. However, certain exigent applications can be worth due to the single-molecule sensitivity [171]. Optical methodologies are far the most explored approach for LoaD platforms due to the cost-effectiveness, the possibility of miniaturisation and personalising of PoC devices, being the closest to fully satisfy the (RE)ASSURED criteria. There are a huge number of publications on optical detection-based LoaD sensors, some of them are summarised in Table 3 to exemplify the variety of detection approaches, analytes, assay types and processes integrated on LoaD biosensors.

Table 3. Summary of some optical detection-based LoaD biosensors. DR: detection range, LOD: limit of detection, WB: whole blood.

Ref	Analyte	Optical Technique (Assay Type)	Total Assay Time	Analytical Data	Comments
[99]	Prostate cancer biomarkers (t-PSA and HER-2)	Absorbance (sandwich and competitive ELISA)	3180 s	LOD: 0.894 ng/mL HER2 and 0.408 ng/mL fPSA	Not tested in real samples.
[164]	Hemoglobin A1c	Absorbance (immunoturbimetry)	8 min	DR: 3.5–12.1 % HbA1c	Input: 1 µL WB 14 samples tested. Standard deviation of 0.36% for each sample (in the order of laboratory equipment)
[172]	Human albumin	Absorbance (sandwich-ELISA)	18 min	LOD: 0.516 ng/mL DR: 0–100 ng/mL	Off-disc absorbance measurement.
[173]	Liver function markers (ALB, TBIL, DBIL, ALP, GGT)	Absorbance (enzymatic assays)	20 min	DR: 0–54.9 µmol/L TBIL, 0–54.9 U/L ALB, 0–48.0 U/L GGT, 0–159 U/L ALP	Input: 150 µL WB All processing integrated in a POC device with wireless communication.
[145]	Dengue NS1 protein	Blu-ray optomagnetic signal (immuno-MNP)	8 min	LOD: 25 ng/mL DR: up to 20,000 ng/mL	Input: 6 µL serum
[146]	Thrombin	Blu-ray optomagnetic signal (immuno-MNP)	15 min 30 s	LOD: 25 pM in PBS	Not tested in real samples.
[110]	C-reactive protein (CRP)	Blu-ray optomagnetic signal (immuno-MNP)	14 min	LOD: 30 µg/mL	Input: 35 µL diluted blood. Dilution performed off-disc.
[91]	Botulinum toxin	Fluorescence (sandwich-immunoassay)	<30 min	LOD: 0.09 pg/mL	Disc placed under microscope
[139]	*Mycobacterium tuberculosis* (TB), *Acinetobacter baumanii* (Ab)	Fluorescence (RTLAMP)	2 h	LOD: 10^3 cfu/mL TB (sputum), 10^2 cfu/mL Ab (blood)	Sputum and WB pre-treatment required. All LAMP processing and detection integrated.
[157]	Avian influenza viruses	Fluorescence (RTLAMP)	70 min	LOD: 25 copies for N3 gene detection	Input: 40 µL WB. All LAMP processing and detection integrated. Wireless communication for temperature control and real time measurement.

Table 3. *Cont.*

[155]	Influenza A virus	Fluorescence (RT-LAMP)	47 min	LOD: 10 copies of RNA	Sample from nasal swabs. 10-fold higher sensitivity than conventional RT-PCR. All LAMP protocols and detection integrated.
[90]	Hepatitis B virus	Fluorescence (PCR)	48 min	LOD: 10^2 copies/mL	Input: 500 µL WB. All PCR protocols and detection integrated.
[174]	Model IgG	Fluorescence (sandwich-ELISA)	62 min	LOD: 20 ng/mL	Disc placed under microscope
[175]	C-reactive protein (CRP) and cardiac troponin I (cTnI)	chemiluminescence (sandwich-ELISA)	30 min	CRP in serum: LOD: 6.0 fM, DR: 8.0 fM–0.8 pM cTnI in WB: LOD: 1.5 pM, DR: 0.4 pM–4.0 nM	Input: 10 µL WB Chemiluminescence measured with a home-built system.
[87]	Model IgG	SPR (direct immunoassay)	<1h	DR: 0–100 µg/mL LOD: 19.8 µg/mL in PBS	Kretschmann configuratio SPR. Developed to input 600 µL WB (not tested in real samples).

4.4.2. Electrochemical Detection

Electrochemical methods are widely used in conventional off-chip sensors because of the fast response, high sensitivity, and relatively low-cost, however, they have been under explored in LoaD devices. This is related to the complexity in integrating the electrochemical signal transducer to the LoaD platform, which demands electrodes included in the disc, and a potentiostat in direct contact with these electrodes. In other words, this usually implicates that the rotation should be stopped to connect the electric contacts to the disc electrodes to perform the measurement. Nwankire et al. [86] implemented gold electrodes functionalised with capture biomolecules where label-free electrochemical detection methods were deployed for measurement. Whole blood was centrifuged on-board, where the cancer cell rich plasma is extracted via a siphon microchannel. Centrifuge-pneumatic DF valves control the realise of reagent for the assay to be carried out. Five identical testing sites exist on the electrochemical-LoaD, allowing for multiple assays being carried out in parallel. The disc was stopped to Electrochemical Impedance Spectroscopy (EIS) measurement for each compartment invidually. The device boasts an 87% capture efficiency over a dynamic range of three orders of magnitude with a lower LOD of 214 cells/mm^2. The lower LOD equates to just 2% of the total working electrode surface [86]. The detection method of label-free EIS allowed for rapid cancer cell detection. The change in the electrical interfacial properties of the surface due to biological binding events is detected. For label-free detection, the changes in the dielectric constant, resistance and capacitance on the surface due to the capture of the target molecule is measured. The change in the impedance would be an indication of whether an analyte has been captured or not, and depending on the change, whether it is a high or low concentration of the target analyte.

Electrochemical biosensors of this nature have attracted major interest for label-free analysis as they don't require as many assay steps as their labelled counterpart for signal acquisition. This form of biosensing attains sensitivity and simplicity which makes them a reliable, quantifiable diagnostic tool for whole cell capture and detection [176]. Opting for whole cell detection rather than DNA detection also reduces the cost and time of detection, as no cell lysis or additional reagents are necessary. The use of sputter-coated electrodes allows for the platform to be disposed of after a single-use and more cost effective, making this type of PoC device economical. These results give a true insight into the huge potential that exists for electrochemical-LoaDs as they are an efficient prognostic devices where minimal sample preparation is required and can be further developed for clinical applications [86]. The relative changes in impedance (difference between values of the anti-EpCAM coated gold electrodes before and after interaction with different concentrations of SKOV3 cells) varies linearly with the captured cell number [86].

To overcome the drawback concerning the integration of the detection system, recent works have focused on the electrochemical modules to allow measurements during the disc rotation [25,153]. This opening up opportunities of real-time monitoring of bioreactions on disc [25,153]. Andreasen et al. [25] developed a low-noise component (electrical slip-ring) to on-disc electrochemical measurements. Cyclic voltammetry tests performed from 0–600 RPM indicated only a small perturbation of the peak currents with the spin rate. Recently, Rajendran et al. [153] demonstrated a modular lightweight (127 g) and wireless potentiostat-on-a-disc (PoD) able to perform square-wave voltammetry (SWV) and amperometry, controlled by a custom-made software. The current resolution of 200 pA was in agreement with commercial potentiostats. During the experiment, data was transmitted via Bluetooth to a Windows PC, plotted live and displayed in a custom-developed LabVIEW program (Figure 12A). The PoD detection unit was composed by a Qi-based wireless power supply, a core circuit platform and a module (shield) (an exploded view in Figure 12B). Figure 12C(a) presents the cyclic voltammograms (CV) of 1 mM potassium ferricyanide (FiC) collected in stationary-mode using the PoD and a commercial potentiostat and (b) CVs collected in different spinning rates by the PoD. At 0 and 1 Hz, the reaction was diffusion-limited while reaction-limited (due to the mass transfer) at 2 Hz and above [153]. The comparison between PoD and the commercial equipment was extended to SWV: (c) voltammograms of 10 mM ascorbic acid and (d) the respective calibration

curve. Both cyclic voltammetry and SWV measurements obtained by the PoD were comparable to the commercial system. The dependence of the amperometric response with the spin rate was tested in a multichannel shield, shown in (e), with the current response for 500 µM FiC increasing with the rotation frequency, as observed in current *versus* FiC concentration plot, shown in (f). Refer to the source for details [153].

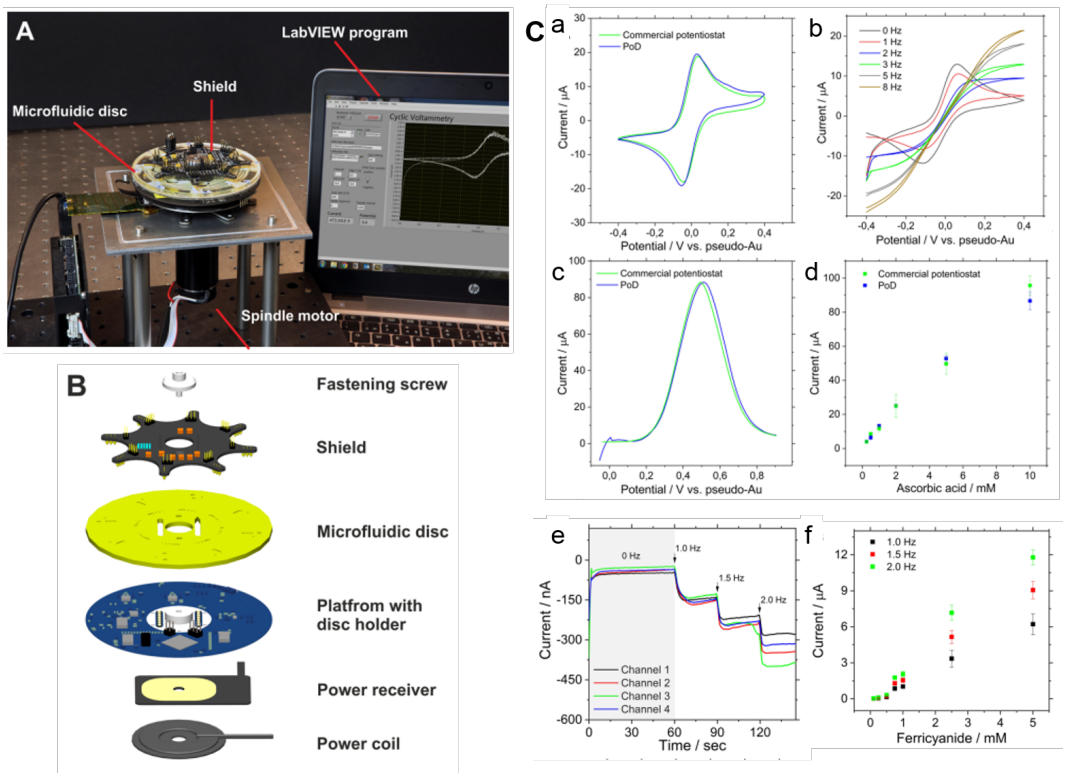

Figure 12. (**A**) Photograph of the experimental set-up with the spindle motor, LoaD platform, PoD and computer to control the software interface. (**B**) Exploded view of the PoD and LoaD device. (**C**) PoD results: (**a**) CVs of 1 mM FiC (Au working electrode with area of 50 mm^2, scan rate of 50 mV/s comparing PoD and commercial potentiostat results, and (**b**) CVs collected in various rotation speeds at scan-rate of 100 mV/s; (**c**) SWVs of 10 mM ascorbic acid (carbon working electrode with 50 mm^2, potential step 0.004 V, frequency of 10 Hz and amplitude of 0.025 V), and (**d**) calibration curve for ascorbic acid concentrations. (**e**) Amperometric response for 500 µM FiC (pH 7.4 PBS as supporting electrolyte, applied potential of −0.4 V *vs* pseudo-Au reference electrode; working electrode area: 0.69 mm^2; Au counter-electrode) in different rotation speeds, and (**f**) the normalised current changes recorded for different FiC concentrations during rotation at 1.0, 1.5, and 2.0 Hz (n = 3). Adapted with permission from [153]. Copyright 2019 American Chemical Society.

Sanger et al. [177] report a centrifugal platform capable of capturing and sensing pathogens. The robust LoaD contains an integrated sample pre-treatment system where SWV are used for cell free detection of a secondary metabolite, p-Coumaric acid (pCHA), a biomolecule produced by genetically modified strains of E-Coli bacteria. A common attribute of LoaD platforms is their ability to contain multiple, identical testing sites. A total of eight regions are available for individual biosensing, where a 0.2 µm filter membrane system exists in each section for sample filtration. This filtration and separation occur under centrifugal conditions for 5 min at approximately 12 Hz. The supernatant is metered and then displaced into the detection chamber. Unlike other electrochemical-LoaDs, the sensors are patterned onto an acrylic base of the platform using e-bean evaporation. Contact points connecting both potentiostat and sensor exist through the depth of the LoaD to establish a connection through a slip-ring. Measurements are obtained under static conditions and showed very promising results for

the detection and quantification of the two E. coli pCHA metabolites compared to results obtained from other detection methods such as HPLC [152].

This group also reported a novel, on-board pre-treatment based on supported liquid membrane (SLM) technology. This extraction method is used to purify and enrich analytes directly from complex matrices such urine and saliva [23,49]. Using the SLM to facilitate on-disc separation, the main hindering compound, Tyrosine, is subsequently removed and the pCHA is enriched. The platform enables multiple measuremtns to be obtained at certain stages of the production process when the target analyte is quite low (typically 100 µM). The main biosensing technique deployed were CV and SWV measurements. As the device is deemed as low-cost it was aimed to be a single use device, however it has been shown that the device can be re-used using typical electrode cycling to clean the surfaces. This work poses a significant insight into the exciting advantages and potential of on-disc sample pre-treatment and electrical detection for analytes in a compact, portable testing [152].

Amperometry is another electrochemical technique where the current response due to a redox on the surface of the biosensor is measured over a period of time at a constant potential [178,179]. It is often used as a detection technique when coupled with electrochemical-LoaD platforms. The potential is maintained at the working electrode via the reference electrode where the current is recorded due to oxidation or reduction of electroactive species. In cases where the analyte is not electrochemically active, the target cannot be measured directly but indirect approaches can be used. Screen-printed carbon electrodes (SPCE) which were modified using graphene-polyaniline nanocomposites were incorporated onto a LoaD to enhance electrochemical detection of glucose. The enzyme and glucose solutions, loaded into separate chambers, mix in a serpentine channel under centrifugal conditions creating the hydrogen peroxide through the enzymatic reaction in under 8 min. The electrochemically active hydrogen peroxide was quantified to deduce the amount of glucose present in the sample, with a reported LOD of 0.29 mM [152]. Common interfering compounds ascorbic and uric acid were tested where the sensor remained specific towards glucose. This is a critical attribute of a biosensor, as it is important to determine to working capability of the sensor for real applications.

Li et al. [180] created a whole blood (WB) analysis system with a primary functionality of performing basic metabolic testing. Different concentrations of glucose, uric and lactate acids in WB spiked samples were analysed within minutes [180]. WB is a very difficult medium to work with, as various blood components non-specifically bind to sensor surfaces. Figure 13(A) depicts the design of one of the testing sections comprising a microfluidic layer, an insulating layer an a biosensing layer. The system set-up contains a nano-porous Au plated Si electrode. Carbon nanotubes on the working electrode increases the electrode surface area which increases the rate of immobilisation of Prussian blue (catalyst) and the analytes. Sample sizes of just 16 µL was required to perform each test, where each PDMS device contained eight individual testing sites. Amperometry allowed for rapid detection and LODs of 0.3 mM of glucose, 0.1–0.2 mM of uric acid and 0.7–1.5 mM. Figure 13(B) illustrates (a) the WB sample loaded. The centrifugation of the WB samples separates the blood components and plasma for analyte capture and electrochemical detection, as illustrated in (b). To further verify the capabilities of the device, a comparison study was carried out using a commercial colorimetric assay, where results indicated deviations for glucose, lactate and uric acid of 4.2%, 5.2% and 6.0%, respectively, between both methods [180].

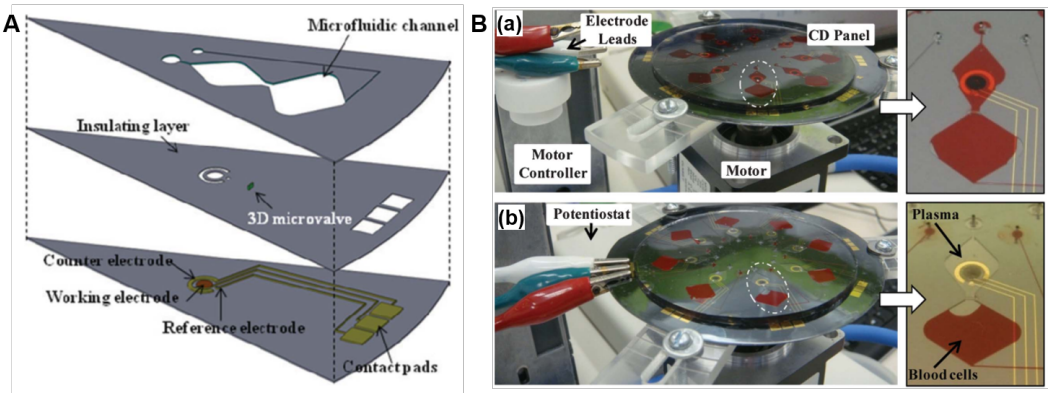

Figure 13. (**A**) Conceptual design of one of eight testing sites displaying each consecutive layer of the PDMS electrochemical-LoaD: a microfluidic layer, an insulating layer and a biosensing layer. (**B**) Electrochemical-LoaD whole blood analysis: (**a**) sample loaded ready for rotation, and (**b**) sample centrifuged and the plasma isolated for measurement of electrochemical signal. Reproduced from [180] with permission from The Royal Society of Chemistry.

Amperometry on a LoaD was again reported by Kim et al. [23] where the cardiac marker, C-reactive protein (CRP), was detected in 20 min. The on-board ELISA assay detected using gold electrodes, fabricated using E-beam lithography. 300 Å of chromium was deposited acting as an adhesion layer, followed by deposition of 3000 Å of gold to create the desired electrode pattern for the electrical connection [181]. Ferrowax valves allows for on-board reagent storage which are actuated using a mobile laser under static conditions [37]. The CRP LOD for this system was 4.9 pg/mL, a 17-fold improvement in quantification by optical density (OD) which is the standard ELISA detection method. This device adds to the very small research bracket of microfluidic-electrochemical crossovers for successful detection for very low concentrations of biomarkers.

5. Biosensing on Existing and Emerging Commercial Point-of-Care Lab-on-a-Disc Devices

Among the first companies to offer a LoaD platform on the market was Abaxis with the Piccolo Xpress [182]. In 1995 they launched the Primary Health Panel (a nine-test reagent disc), and the General Health Panel (a 12-test reagent disc). The Liver Panel Plus arrived the next year. Nowadays, Abaxis offers fast blood analysis (about 12 min) with 31 tests across 16 complete chemistry panels [182]. Thenceforth, other assays became available, as the PCR-based devices from Revogene Platform by Meridian Bioscience [183] (tests for gastrointestinal conditions, pediatric and neonatal conditions, respiratory conditions and enterobacteria infection), and the Simplexa assays to be run in 3M Integrated Cycler [184] (real-time PCR for quantitative and multi-analyte detection of virus infections, as well as to develop extraction and amplification assays using the kits the company offers in its catalog) .

Strohmeier et al. [34] presented a complete list of companies selling LoaD platforms until 2015 in a review paper. On this occasion, Hahn-Schickard [185] was cited as in the development stage. Today, this German company operates as an R & D service provider, developing solutions in microsystem technology, with a wide portfolio of services. Recently, Hahn-Schickard and related company Spindiag GmbH jointly received an investment of 6 million Euros from the German government to establish a SARS-CoV-2 virus rapid test to address COVID-19 [186] based upon their existing platforms. Spindiag [187] is a medical technology specialised start-up founded in 2016 as a spin-off of the Hahn-Schickard. In May 2020, Spindiag announced an additional 16.3 million Euros investment to prepare market launch of the Rhonda mini-lab for SARS-CoV-2 virus. The Rhonda system is a PCR-based device and will provide results in 30–40 min with minimal contact between the operator and sample. Swab samples from the nose and throat are directly inserted into the cartridge, which contains all the required reagents. The system is on an analytical test and it is expected to receive

market approval in Germany and European Union during the third quarter 2020 (information from Spindiag website [187]).

Immunoassays often require multiple steps such as sample incubation, washing and elution steps, blood separation and a final detection output. Gyros ABTM has proven commercial success with a first-generation centrifugal testing platform for immunoassay applications. The platform uses hydrophobic regions to regulate the sequential flow inside the injection moulded device which permits on-board metering and aliquoting of reagents. One device provided by the company, Gyrolab Bioaffy CD [188], has up to 112 channels which allows for high throughput testing of the sample where the users own specific biomarker may be detected. The device contains a series of metering structures, which evenly distributes the capture reagent. Streptavidin coated beads in each region are incubated with the capture biomolecules, where the excess reagent is displaced into another chamber by increasing the spin frequency of the platform. Samples, of 200 nL defined volume, enter the incubation area by capillary action where the analyte is captured. A secondary detection reagent is then passed through the capture column, creating a sandwich assay. This nanolitre immunoassay significantly reduces sample and reagent usage where fluorescence detection from the assay is reportedly obtained within the hour. The unique selling point of the device is that specific immunoassay can be designed for implementation on the device based on the required dynamic range and analyte concentration where the company itself will provide support whilst designing the LoaD assay. Ghosh et al. [189] reported using the commercially available Bioaffy 1000 CD to measure protein drugs capable of neutralises vascular endothelial growth factor to save patient vision with retinal vascular diseases. Cynomolgus ocular final concentrations were determined using an Alexafluor labelling kit and where visualisation and measurements were achieved using laser-induced fluorescent detection at a 647 nm wavelength [189]. Many advantages are offered by this device regarding assay volume sizes being realised with this platform, there are many clear drawbacks with the concept. The company does not provide with ready to use devices, where all biorecognition molecule pairs for the sandwich assay require specific user knowledge. As the assay detects biomolecules, some form of sample preparation is required which cannot be performed on the LoaD [34,190].

The LabGEO IB10 device is commercially available centrifugal platform distributed by Samsung. The device is an integrated system that combines a microfluidic platform and an analyser for cardiac biomarker detection from whole blood. This LoaD only requires 500 µL of a whole blood sample from the user, where all other reagents are pre-loaded. Proteins such CK-MB, Troponin and Myoglobin are extracted from whole blood and tested within 20 min where an optical density ranging over 10 specific wavelengths are obtained by the accompanying centrifuge analyser platform [191]. The platform contains freeze-dried reagents for blood chemistry analysis. The fluid flow is controlled using laser actuated ferrowax microvalves to activate specific reagent steps for the assay. All samples processing is carried out automatically. Other commercial LoaDs have combined both testing and optical density analysis conjoined system [154] however, Samsung appear to be the only competitors on the current market which have been able to provide analysis using whole blood analyte extraction on a PoC system.

Another example of an optical detection system is the ViroTrack® cartridge produced by BluSense Diagnostics (Denmark). Although the chip is not a LoaD by definition, it is a segment which operates using centrifugal microfluidic technology. The ViroTrack® is a single use cartridge which provides results with just one drop of blood in 10 min. The assay technology contained within the chip uses magnetic nanoparticles (MNPs) coated with capture biomolecules that will react and capture the specific target. These MNPs are released which bind with the target biomolecule within the blood. After the incubation period, a strong magnetic field aggregates with MNPs where the density of these are subsequently measured by the BluBox instrument to produce semi-quantitative results. Various versions of the chip are available to test for Dengue, Zika and Chikungunya, Covid-19 viruses [192,193].

Although there are already some LoaD platforms on the market, there is still room for extensive research into new devices. Researchers from University of Freiburg developed a disposable ready-to-use microfluidic cartridges (termed GeneSlices) for PCR assays [194,195]. Four GeneSlice

cartridges were fit in a custom made rotor replacing the standard rotor in a commercial Rotor-Gene (Qiagen, Germany) [194,195]. In collaboration with Hahn-Schickard, they created an automated PCR-based disc for bacterial pathogen detection to run on a portable LabDisk-player [137] with a minimal manual step since the reagents and buffers were pre-stored in stick-packs [94]. Pathogens detection via LAMP nucleic acid amplification have been also developed [196,197]. An extreme PoC device for malaria field detection was based on a real-time LAMP assay in a compact analyzer and a disposable microfluidic compact disc. The device was capable to process 4 samples simultaneously within 50 min, with a material cost ~$1/test, and achieving a LOD of 0.5 parasites/µL whole blood (sufficient to detect asymptomatic parasite carriers) [196].

One of the most promising LoaD devices is in the field of circulating tumor cells (CTC). In 2014, Professor Cho's group from Ulsan National Institute of Science and Technology (UNIST) suggested a LoaD platform for CTC isolation by mechanical filtration. The size-selective CTC detection system used a commercially available track-etched polycarbonate membrane with 8 µm-pore-size, specially chosen based on the size of the CTC. The entire process of CTC isolation, staining and detection was integrated on disc by a programmable operating system. When compared to the commercial ScreenCell, the caption efficiency for the MCF-7 cells was slightly lower (56 ± 2% compared to 69 ± 6%) (n = 3), however, the contamination by white blood cells was 20-fold lower with the disc system [198]. In 2017, they suggested the fluid-assisted separation technology (FAST) for CTC isolation using the same filter but now with the pores filled with a stably held liquid during the entire filtration process, achieving an impressive recovery rate of 95.9 ± 3.1% [199]. While in a non-FAST mode, the filtration left the majority of particles located in the outer rim of the filter (only a small part of the filter is used), the membrane fully wet before and during the filtration process allows the liquid transport at a pressure lower than the capillary pressure, leading to a uniform filtration throughout the entire membrane [116]. The FAST device was successfully validated in a pre-clinical test in unprocessed whole blood of 40 patients with non-small cell lung cancer [116]. FAST disc was patented, licensed to Clinomics [200] (Ulsan, Korea). A pilot study using the FAST device was performed in whole blood of 13 patients with ovarian cancer, for isolation and enumeration of CTC, and to assess the correlations among CTC, cancer antigen-125 levels and the clinical course of the disease [201]. The FAST disc presents great potential to provide minimally invasive way to detect metastasis and for monitoring treatment response in patients.

Through technological advances, the current wireless technology and Bluetooth connectivity can allow the complete automation of processes on disc. Besides the control of spinning protocols, important experimental parameters, as valve action and temperature control [202], as well as real-time data acquisition [141,153,154,203–205] can be performed by Bluetooth connection. To avoid stopping the disc and/or off-disc measurements, an electrified-LoaD (eLoaD) platform [203,204] was created to allow continuous measurement while the disc is spinning with data transmission via Bluetooth, which has special importance for time-dependent reactions and biochemical reaction kinetics. The platform is assembled on a modular set-up, with an interchangeable and non-disposable "application disc" specifically designed for the intended application, sandwiched between the LoaD microfluidic disc (top) and the eLoaD platform (bottom). Authors highlighted the versatility by adapting the "application disc" to the intended protocol, for instance, manufacturing an "application disc" for optical detection by housing proper set of LEDs and photodetectors, or by housing a set of temperature sensors and heaters to automate the temperature control, etc. [204]. The wireless power is transferred during the disc rotation from a 5 W-Qi Standard transmitter, commonly used to charge smartphones. An Arduino microcontroller, a Bluetooth communication module and an SD-card module are settled in the platform [204]. The portability and the easy control by Tablets and Smartphones can be a key feature for extreme PoC devices, and for daily diagnostics for a rapid data transfer to health care professionals by remote consultation.

Technological advances in materials processing and digital innovations (mobile-health and internet of things) have contributed to create diagnostic tests to satisfy (or nearly satisfy) the REASSURED criteria for PoC devices [31].

- **R**eal-time connectivity: Wireless Bluetooth connectivity in LoaD has allowed both operation control and result visualisation [26,154,161,202,204]. It can be implemented to allow that the results are rapidly provided to the patient as soon as the test is completed.
- **E**ase of specimen collection and **E**nvironmental friendliness: It is preferable that tests with blood utilise small volumes to allow self-collection using finger stick kits. The blood processing is easily integrated on disc rather than any other microfluidic separation strategy. Some tests can be less invasive using swabs for sample collection (vaginal, nasal, oral) allied to PCR detection [32]. The environmental point-of-view draws attention to the cumulative effect and environmental risks concerning the disposal of contaminated discs. Although often neglected in the published works, it is time to start considering the recyclability of materials in the manufacture of the biosensors. The viability of small interchangeable cartridges to contaminated solutions could eventually allow the correct disposal of the contaminated residues (incineration), while a great part of the disc can be directed for recycling.
- **A**ffordable tests can be achieved thanks to the relatively cheap and easy processing of polymers and possible scale production. Certainly, the most expensive parcel of the total cost of a biosensor is related to the biochemical reagents, which also implicate in additional costs in special storage and transport conditions.
- **S**ensitive and **S**pecific LoaD biosensors have been reported for various analytes. The first is provided by the combination of sensitive detection methods and well-done sample processing (reduced background noise) while the second is provided by the biospecificity of the biorecognition element (enzyme–substrate or antigen–antibody specificity and nucleic acid sequences complementarity).
- **U**ser friendliness: LoaD biosensors can be implemented to satisfy this criterion since all the disc processing and data collection and analysis can be automated, starting with a single "play" bottom push.
- **R**apid and **R**obust tests: LoaD can address these criteria. For example, LoaD immunoassays were completed with significantly reduced assay time compared to common benchtop ELISA (blood separation time reduced to about 8 min while sample incubation is successfully achieved in 10 min [87,99]). Concerning robustness, some disc designs allow the placement of the biosensing surface to the disc just immediately before the test, facilitating disc fabrication and avoiding special transport and storage conditions [87].
- **E**quipment-free and **D**eliverable: Inexpensive discs can be manufactured and easily delivered, the need for equipment including programable rotation motor and detection system still keep the LoaD technologies restricted to laboratory walls. For this reason, LoaD diagnostic tests in the market still target the diagnostic laboratories and are not available as self and home tests.

6. Future Perspective of Biosensing Platforms

Biosensing LoaDs performing bio-assays often requires complex sample processing with an increased level of integration, making them robust and effective tools in PoC testing. Advancements have been made in LoaD manufacturing and fabrication strategies in the past decade, however significant challenges are prevalent for the successful integration of microfluidic PoC systems into routine clinical diagnosis [206]. One of the main challenges for centrifugal microfluidics to become commercially desirable is extending the shelf life of the PoC device. For biosensing and assay performance, multiple reagents are necessary for testing. For these platform to remain highly attractive products on the market, the LoaDs must be semi/fully automated. This attribute is dependent on multiple factors, including;

1. On-board reagent storage: The requirement of assay reagents has limited the development of clinical microfluidic devices, however advancements have been made in recent years to combat this issue. Reagents can be integrated and stored within LoaDs in a variety of ways. Dry reagent storage in can be achieved through inkjet printing and lyophilisation [207,208]. Dehydration of the compounds often impedes the degradation of the reagents and therefore increases the shelf life of the devices in varying environments. This in turn allows for mass manufacturing and storage of the platforms. This will allow for already existing biological assays to be implemented onto the centrifugal platform as a ready-to-use diagnostic tool [209].
2. Reagent actuation: Nucleic acid analysis is a multi-step assay, consisting of cell lysis, nucleic acid enrichment and amplification, and signal readout. The integration of these types of assays calls for clever microfluidic engineering for sequential reagent actuation which can be offered by laser, electro, photo and centrifugal induced pressure triggering valves, siphons and graphene oxide valves for fluid specific routing of liquids [210–212]. This allows the devices to become "ready-to-use" tests within a clinical setting. The majority of these options have existed for some time, however, within the last decade, research groups are now putting an emphasis on inventing specific µTAS [213]. Interdisciplinary groups are innovating LoaDs with complementary detection systems built around the architecture of the diagnostics platform. Previously discussed literature has proven the value of this type of integration i.e., centrifuges with built in heating blocks for rapid PCR assays [214], optics for optical density and fluorescence detection [90] and modular wireless potentiostat-on-a-disc for electrochemical detection [153]. These systems have only become evident in recent years and are becoming increasingly popular within literature. This trend is expected to grow in the next coming years. BluSense Diagnostics have already reached commercial success by offering a centrifugal style chip requiring one droplet of blood to carry out the disease diagnostics tests on their custom centrifuge analyser system [215].
3. Nanotechnology integration: Nanotechnology fabrication techniques have also significantly advanced in recent years, which are now being implemented into PoC devices for more specific detection of analytes. Deployment of nanoparticles coated with specific antibodies/antigens, magneto-nanoparticles, micropillar structures, Au cavities and AuNPs are deployed within centrifugal sensing platforms are reporting greater sensitivity which rivals that of gold-standard assays currently used [216,217]. The nanostructures deployed during testing are more specific towards the analyte and therefore reduces the LOD. As well as the greater sensitivity offered by nanostructures they also assist in overcoming standard microfluidic phenomena. Bioassays require adequate mixing of various phases (liquid, silica beads, etc.) which is difficult to achieve in microfluidic platforms due to the low Reynolds number of liquids in reservoirs and channels. Materials and techniques are now being explored thanks to developments in nanotechnology fabrication. Micropillars and other structures created using lithographic and additive manufacture techniques can disrupt laminar flow in channels, creating the desired mixing motion necessary for these assays [218]. This will need to be explored in the future, however presently these are considered complex manufacturing processes and would be difficult to mass manufacture for commercial success.
4. Additive Manufacturing: The availability of high resolution 3D printing techniques to researchers may facilitate the fabrication and mass production of particularly complicated LoaD design with minimal variation between batch production, making assay performance repeatable and reliable [219,220]. Advances with materials and technologies paired with clever design and fabrication of LoaDs may make laborious clinical application of microfluidics achievable in the near future.

7. Final Remarks

In search of complementarity between microfluidics and biosensing, the centrifugal microfluidic platform has emerged as an preeminent platform of significant interest to academic researchers

and commercial enterprises. The key advantage is the capability of the LoaD to enable transfer of LUOs (pipetting, metering, mixing etc.) directly from the conventional lab "wet bench" to "on disc" while requiring minimial protocol changes or optimisation. This ease of automation results in faster and more robust assay development compared with other emerging PoC platforms, such as paper microfluidics [221], where advantages such as greater deployability (for example not requiring a spindle motor to function) are counterbalanced by a greater upfront burden of assay development or biosensor optimisation. Furthermore, the LoaD platform is continuously evolving and has been shown to be a platform which can be adapted to leverage the latest emerging technologies (such as the Arduino controllers and wireless mobile-phone charging technology described above). Every year new LoaD automation and biosensing technologies have been developed to demonstrate sample-to-answer PoC biodetection with minimal user interaction. Even with devices already commercialised, there is plenty of space for researchers to develop the LoaD with new technologies to address new challenges. We hope this review paper has provided researchers interested in working in this field a comprehensive overview of the recent advances on LoaD biosensors.

Author Contributions: Writing—original draft preparation, C.M.M., E.C., and D.J.K.; writing—review and editing, C.M.M., E.C., and D.J.K. All authors have read and agreed to the published version of the manuscript.

Funding: Sao Paulo Research Foundation grants 2014/15093-7 and 2015/16311-0 and partly funded by Enterprise Ireland under Grant No. CF/2019/1080.

Conflicts of Interest: The authors declare no conflict of interest.

Abbreviations

The following abbreviations are used in this manuscript:

COP	Cyclic olefin polymer
CRP	C-Reactive Protein
CTC	Circulating Tumor Cells
CV	Cyclic Voltammogram
DF	Dissolvable Film
DGM	Density Gradient Medium
DNA	Deoxyribonucleic Acid
eLoaD	electrified-Lab-on-a-Disc
EDC	N-(3-dimethy-laminopropyl)-N -ethylcarbodiimide hydrochloride
EIS	Electrochemical Impedance Spectroscopy
ELISA	Enzyme-Linked Immunosorbent Assay
FAST	Fluid-Assisted Separation Technology
FiC	Potassium ferrycyanide
FLISA	Fluorescence-Linked Immunosorbent Assay
HBV	Hepatitus B Virus
ID	Individually Addressable Diaphragm
IVD	In Vitro Diagnostics
LAMP	Loop-mediated Isothermal Amplification
LED	Light Emitting Diode
LoaD	Lab-on-a-Disc
LOD	Limit of Detection
LUO	Laboratory Unit Operations
MNPs	Magnetic Nanoparticles
µTAS	micro-Total Analysis System
NASBA	Nucleic Acid Sequence-Based Amplification
NHS	N-hydroxyuccinimida
OD	Optical Density
PCR	Polymerase Chain Reaction
PEI	Poly(ethylene imine)

PMMA	Poly(methylmethacrylate)
PoC	Point-of-Care
PoD	Potentiostat-on-a-Disc
RBC	Red Blood Cells
RPA	Recombinase Polymerase Amplification
SLM	Supported Liquid Membrane
SPCR	Screenprinted Carbon Electrode
SPR	Surface Plasmon Resonance
SWV	Square-wave voltammetry
TOS	Triangle Obstacle Structure
WB	Whole blood

References

1. Nagel, B.; Dellweg, H.; Gierasch, L. Glossary for chemists of terms used in biotechnology (IUPAC Recommendations 1992). *Pure Appl. Chem.* **1992**, *64*, 143–168. [CrossRef]
2. Reddy, S.M.; Paixão, T.R.L.C. *Materials for Chemical Sensing*; Springer: Berlin/Heidelberg, Germany, 2017; p. 268. [CrossRef]
3. Whitesides, G.M. The origins and the future of microfluidics. *Nature* **2006**, *442*, 368–373. [CrossRef] [PubMed]
4. Tian, W.C.; Finehout, E. Introduction to microfluidics. In *Microfluidics for Biological Applications*; Springer: Berlin/Heidelberg, Germany, 2008; pp. 1–34.
5. Madou, M.; Zoval, J.; Jia, G.; Kido, H.; Kim, J.; Kim, N. Lab on a CD. *Annu. Rev. Biomed. Eng.* **2006**, *8*, 601–628. [CrossRef] [PubMed]
6. Analytics, C. Web of Science. Available online: www.webofknowledge.com (accessed on 18 May 2020).
7. Kung, Y.C.; Huang, K.W.; Chong, W.; Chiou, P.Y. Tunnel Dielectrophoresis for Tunable, Single-Stream Cell Focusing in Physiological Buffers in High-Speed Microfluidic Flows. *Small* **2016**, *12*, 4343–4348. [CrossRef] [PubMed]
8. Chuang, C.H.; Chiang, Y.Y. Bio-O-Pump: A novel portable microfluidic device driven by osmotic pressure. *Sens. Actuators B Chem.* **2019**, *284*, 736–743. [CrossRef]
9. Sotoudegan, M.S.; Mohd, O.; Ligler, F.S.; Walker, G.M. Paper-based passive pumps to generate controllable whole blood flow through microfluidic devices. *Lab Chip* **2019**, *19*, 3787–3795. [CrossRef]
10. Glawdel, T.; Ren, C.L. Global network design for robust operation of microfluidic droplet generators with pressure-driven flow. *Microfluid. Nanofluid.* **2012**, *13*, 469–480. [CrossRef]
11. Laschi, S.; Miranda-Castro, R.; González-Fernández, E.; Palchetti, I.; Reymond, F.; Rossier, J.S.; Marrazza, G. A new gravity-driven microfluidic-based electrochemical assay coupled to magnetic beads for nucleic acid detection. *Electrophoresis* **2010**, *31*, 3727–3736. [CrossRef]
12. De Groot, T.; Veserat, K.; Berthier, E.; Beebe, D.; Theberge, A. Surface-tension driven open microfluidic platform for hanging droplet culture. *Lab Chip* **2016**, *16*, 334–344. [CrossRef] [PubMed]
13. Xu, L.; Lee, H.; Jetta, D.; Oh, K.W. Vacuum-driven power-free microfluidics utilizing the gas solubility or permeability of polydimethylsiloxane (PDMS). *Lab Chip* **2015**, *15*, 3962–3979. [CrossRef] [PubMed]
14. Kung, Y.C.; Huang, K.W.; Fan, Y.J.; Chiou, P.Y. Fabrication of 3D high aspect ratio PDMS microfluidic networks with a hybrid stamp. *Lab Chip* **2015**, *15*, 1861–1868. [CrossRef]
15. Luo, Y.; Qin, J.; Lin, B. Methods for pumping fluids on biomedical lab-on-a-chip. *Front. Biosci.* **2009**, *14*, 3913–3924. [CrossRef] [PubMed]
16. Ahmed, D.; Mao, X.; Juluri, B.K.; Huang, T.J. A fast microfluidic mixer based on acoustically driven sidewall-trapped microbubbles. *Microfluid. Nanofluid.* **2009**, *7*, 727. [CrossRef]
17. Ter Schiphorst, J.; Saez, J.; Diamond, D.; Benito-Lopez, F.; Schenning, A.P. Light-responsive polymers for microfluidic applications. *Lab Chip* **2018**, *18*, 699–709. [CrossRef] [PubMed]
18. Fan, Y.; Wu, Y.; Chen, Y.; Kung, Y.C.; Wu, T.; Huang, K.; Sheen, H.J.; Chiou, P.Y. Three dimensional microfluidics with embedded microball lenses for parallel and high throughput multicolor fluorescence detection. *Biomicrofluidics* **2013**, *7*, 044121. [CrossRef] [PubMed]

19. Gilmore, J.; Islam, M.; Martinez-Duarte, R. Challenges in the use of compact disc-based centrifugal microfluidics for healthcare diagnostics at the extreme point of care. *Micromachines* **2016**, *7*, 52. [CrossRef]
20. Huang, Y.; Wang, J.; Zhang, M.; Zhu, M.; Wang, M.; Sun, Y.; Gu, H.; Cao, J.; Li, X.; Zhang, S.; et al. Matrix-assisted laser desorption/ionization time-of-flight mass spectrometry for rapid identification of fungal rhinosinusitis pathogens. *J. Med. Microbiol.* **2017**, *66*, 328–333. [CrossRef]
21. Kinahan, D.J.; Kearney, S.M.; Kilcawley, N.A.; Early, P.L.; Glynn, M.T.; Ducree, J. Density-gradient mediated band extraction of leukocytes from whole blood using centrifugo-pneumatic siphon valving on centrifugal microfluidic discs. *PLoS ONE* **2016**, *11*, e0155545. [CrossRef]
22. Van de Groep, K.; Bos, M.P.; Varkila, M.R.; Savelkoul, P.H.; Ong, D.S.; Derde, L.P.; Juffermans, N.P.; van der Poll, T.; Bonten, M.J.; Cremer, O.L.; et al. Moderate positive predictive value of a multiplex real-time PCR on whole blood for pathogen detection in critically ill patients with sepsis. *Eur. J. Clin. Microbiol. Infect. Dis.* **2019**, *38*, 1829–1836. [CrossRef]
23. Kim, T.H.; Abi-Samra, K.; Sunkara, V.; Park, D.K.; Amasia, M.; Kim, N.; Kim, J.; Kim, H.; Madou, M.; Cho, Y.K. Flow-enhanced electrochemical immunosensors on centrifugal microfluidic platforms. *Lab Chip* **2013**, *13*, 3747–3754. [CrossRef]
24. Noroozi, Z.; Kido, H.; Madou, M.J. Electrolysis-induced pneumatic pressure for control of liquids in a centrifugal system. *J. Electrochem. Soc.* **2011**, *158*, P130. [CrossRef]
25. Andreasen, S.Z.; Kwasny, D.; Amato, L.; Brøgger, A.L.; Bosco, F.G.; Andersen, K.B.; Svendsen, W.E.; Boisen, A. Integrating electrochemical detection with centrifugal microfluidics for real-time and fully automated sample testing. *RSC Adv.* **2015**, *5*, 17187–17193. [CrossRef]
26. Höfflin, J.; Delgado, S.M.T.; Sandoval, F.S.; Korvink, J.G.; Mager, D. Electrifying the disk: A modular rotating platform for wireless power and data transmission for Lab on a disk application. *Lab Chip* **2015**, *15*, 2584–2587. [CrossRef] [PubMed]
27. Martinez-Duarte, R.; Gorkin, R.A., III; Abi-Samra, K.; Madou, M.J. The integration of 3D carbon-electrode dielectrophoresis on a CD-like centrifugal microfluidic platform. *Lab Chip* **2010**, *10*, 1030–1043. [CrossRef] [PubMed]
28. Smith, S.; Mager, D.; Perebikovsky, A.; Shamloo, E.; Kinahan, D.; Mishra, R.; Torres Delgado, S.; Kido, H.; Saha, S.; Ducrée, J.; et al. CD-Based Microfluidics for Primary Care in Extreme Point-of-Care Settings. *Micromachines* **2016**, *7*, 22. [CrossRef]
29. Glynn, M.T.; Kinahan, D.J.; Ducrée, J. CD4 counting technologies for HIV therapy monitoring in resource-poor settings–state-of-the-art and emerging microtechnologies. *Lab Chip* **2013**, *13*, 2731–2748. [CrossRef]
30. Peeling, R.; Mabey, D. Point-of-care tests for diagnosing infections in the developing world. *Clin. Microbiol. Infect.* **2010**, *16*, 1062–1069. [CrossRef]
31. Land, K.J.; Boeras, D.I.; Chen, X.S.; Ramsay, A.R.; Peeling, R.W. REASSURED diagnostics to inform disease control strategies, strengthen health systems and improve patient outcomes. *Nat. Microbiol.* **2019**, *4*, 46–54. [CrossRef]
32. Bissonnette, L.; Bergeron, M.G. The genePOC platform, a rational solution for extreme point-of-care testing. *Micromachines* **2016**, *7*, 94. [CrossRef]
33. Tang, M.; Wang, G.; Kong, S.K.; Ho, H.P. A Review of Biomedical Centrifugal Microfluidic Platforms. *Micromachines* **2016**, *7*, 26. [CrossRef]
34. Strohmeier, O.; Keller, M.; Schwemmer, F.; Zehnle, S.; Mark, D.; Von Stetten, F.; Zengerle, R.; Paust, N. Centrifugal microfluidic platforms: advanced unit operations and applications. *Chem. Soc. Rev.* **2015**, *44*, 6187–6229. [CrossRef] [PubMed]
35. Ducrée, J.; Haeberle, S.; Lutz, S.; Pausch, S.; von Stetten, F.; Zengerle, R. The centrifugal microfluidic Bio-Disk platform. *J. Micromech. Microeng.* **2007**, *17*, S103. [CrossRef]
36. Gorkin, R.; Park, J.; Siegrist, J.; Amasia, M.; Lee, B.S.; Park, J.M.; Kim, J.; Kim, H.; Madou, M.; Cho, Y.K. Centrifugal microfluidics for biomedical applications. *Lab Chip* **2010**, *10*, 1758. [CrossRef] [PubMed]
37. Kong, L.X.; Perebikovsky, A.; Moebius, J.; Kulinsky, L.; Madou, M. Lab-on-a-CD: A fully integrated molecular diagnostic system. *J. Lab. Autom.* **2016**, *21*, 323–355. [CrossRef] [PubMed]
38. King, D.; O'Sullivan, M.; Ducrée, J. Optical detection strategies for centrifugal microfluidic platforms. *J. Mod. Opt.* **2014**, *61*, 85–101. [CrossRef]

39. Burger, R.; Amato, L.; Boisen, A. Detection methods for centrifugal microfluidic platforms. *Biosens. Bioelectron.* **2016**, *76*, 54–67. [CrossRef] [PubMed]
40. Hugo, S.; Land, K.; Madou, M.; Kido, H. A centrifugal microfluidic platform for point-of-care diagnostic applications. *S. Afr. J. Sci.* **2014**, *110*, 1–7. [CrossRef]
41. Nolte, D.D. Invited Review Article: Review of centrifugal microfluidic and bio-optical disks. *Rev. Sci. Instrum.* **2009**, *80*, 101101. [CrossRef]
42. Kinahan, D.J.; Kearney, S.M.; Dimov, N.; Glynn, M.T.; Ducrée, J. Event-triggered logical flow control for comprehensive process integration of multi-step assays on centrifugal microfluidic platforms. *Lab Chip* **2014**, *14*, 2249–2258. [CrossRef] [PubMed]
43. Clime, L.; Daoud, J.; Brassard, D.; Malic, L.; Geissler, M.; Veres, T. Active pumping and control of flows in centrifugal microfluidics. *Microfluid. Nanofluid.* **2019**, *23*, 29. [CrossRef]
44. Chen, J.M.; Huang, P.C.; Lin, M.G. Analysis and experiment of capillary valves for microfluidics on a rotating disk. *Microfluid. Nanofluid.* **2008**, *4*, 427–437. [CrossRef]
45. Gorkin, R.; Clime, L.; Madou, M.; Kido, H. Pneumatic pumping in centrifugal microfluidic platforms. *Microfluid. Nanofluid.* **2010**, *9*, 541–549. [CrossRef]
46. Siegrist, J.; Gorkin, R.; Clime, L.; Roy, E.; Peytavi, R.; Kido, H.; Bergeron, M.; Veres, T.; Madou, M. Serial siphon valving for centrifugal microfluidic platforms. *Microfluid. Nanofluid.* **2010**, *9*, 55–63. [CrossRef]
47. Godino, N.; Gorkin , R., III; Linares, A.V.; Burger, R.; Ducrée, J. Comprehensive integration of homogeneous bioassays via centrifugo-pneumatic cascading. *Lab Chip* **2013**, *13*, 685–694. [CrossRef]
48. Zhu, Y.; Chen, Y.; Xu, Y. Interruptible siphon valving for centrifugal microfluidic platforms. *Sens. Actuators B Chem.* **2018**, *276*, 313–321. [CrossRef]
49. Park, J.M.; Cho, Y.K.; Lee, B.S.; Lee, J.G.; Ko, C. Multifunctional microvalves control by optical illumination on nanoheaters and its application in centrifugal microfluidic devices. *Lab Chip* **2007**, *7*, 557–564. [CrossRef] [PubMed]
50. Gorkin, R.; Nwankire, C.E.; Gaughran, J.; Zhang, X.; Donohoe, G.G.; Rook, M.; O'Kennedy, R.; Ducrée, J. Centrifugo-pneumatic valving utilizing dissolvable films. *Lab Chip* **2012**, *12*, 2894–2902. [CrossRef] [PubMed]
51. Kinahan, D.J.; Early, P.L.; Vembadi, A.; MacNamara, E.; Kilcawley, N.A.; Glennon, T.; Diamond, D.; Brabazon, D.; Ducrée, J. Xurography actuated valving for centrifugal flow control. *Lab Chip* **2016**, *16*, 3454–3459. [CrossRef]
52. McArdle, H.; Jimenez-Mateos, E.M.; Raoof, R.; Carthy, E.; Boyle, D.; ElNaggar, H.; Delanty, N.; Hamer, H.; Dogan, M.; Huchtemann, T.; et al. "TORNADO"—Theranostic One-Step RNA Detector; microfluidic disc for the direct detection of microRNA-134 in plasma and cerebrospinal fluid. *Sci. Rep.* **2017**, *7*, 1750. [CrossRef]
53. Al-Faqheri, W.; Ibrahim, F.; Thio, T.H.G.; Aeinehvand, M.M.; Arof, H.; Madou, M. Development of novel passive check valves for the microfluidic CD platform. *Sens. Actuators A Phys.* **2015**, *222*, 245–254. [CrossRef]
54. Kazemzadeh, A.; Ganesan, P.; Ibrahim, F.; Aeinehvand, M.M.; Kulinsky, L.; Madou, M.J. Gating valve on spinning microfluidic platforms: A flow switch/control concept. *Sens. Actuators B Chem.* **2014**, *204*, 149–158. [CrossRef]
55. Kinahan, D.J.; Renou, M.; Kurzbuch, D.; Kilcawley, N.A.; Bailey, É.; Glynn, M.T.; McDonagh, C.; Ducrée, J. Baking powder actuated centrifugo-pneumatic valving for automation of multi-step bioassays. *Micromachines* **2016**, *7*, 175. [CrossRef] [PubMed]
56. Cai, Z.; Xiang, J.; Zhang, B.; Wang, W. A magnetically actuated valve for centrifugal microfluidic applications. *Sens. Actuators B Chem.* **2015**, *206*, 22–29. [CrossRef]
57. Cai, Z.; Xiang, J.; Wang, W. A pinch-valve for centrifugal microfluidic platforms and its application in sequential valving operation and plasma extraction. *Sens. Actuators B Chem.* **2015**, *221*, 257–264. [CrossRef]
58. Aeinehvand, M.M.; Weber, L.; Jiménez, M.; Palermo, A.; Bauer, M.; Loeffler, F.F.; Ibrahim, F.; Breitling, F.; Korvink, J.; Madou, M.; et al. Elastic reversible valves on centrifugal microfluidic platforms. *Lab Chip* **2019**, *19*, 1090–1100. [CrossRef] [PubMed]
59. Xiang, J.; Cai, Z.; Zhang, Y.; Wang, W. Wedge actuated normally-open and normally-closed valves for centrifugal microfluidic applications. *Sens. Actuators B Chem.* **2017**, *243*, 542–548. [CrossRef]
60. Aeinehvand, M.M.; Martins Fernandes, R.F.; Jiménez Moreno, M.F.; Lara Díaz, V.J.; Madou, M.; Martinez-Chapa, S.O. Aluminium valving and magneto-balloon mixing for rapid prediction of septic shock on centrifugal microfluidic platforms. *Sens. Actuators B Chem.* **2018**, *276*, 429–436. [CrossRef]

61. Kim, T.H.; Sunkara, V.; Park, J.; Kim, C.J.; Woo, H.K.; Cho, Y.K. A lab-on-a-disc with reversible and thermally stable diaphragm valves. *Lab Chip* **2016**, *16*, 3741–3749. [CrossRef]
62. Duffy, D.C.; McDonald, J.C.; Schueller, O.J.; Whitesides, G.M. Rapid prototyping of microfluidic systems in poly (dimethylsiloxane). *Anal. Chem.* **1998**, *70*, 4974–4984. [CrossRef]
63. Xia, Y.; McClelland, J.J.; Gupta, R.; Qin, D.; Zhao, X.M.; Sohn, L.L.; Celotta, R.J.; Whitesides, G.M. Replica molding using polymeric materials: A practical step toward nanomanufacturing. *Adv. Mater.* **1997**, *9*, 147–149. [CrossRef]
64. Gale, B.K.; Jafek, A.R.; Lambert, C.J.; Goenner, B.L.; Moghimifam, H.; Nze, U.C.; Kamarapu, S.K. A review of current methods in microfluidic device fabrication and future commercialization prospects. *Inventions* **2018**, *3*, 60. [CrossRef]
65. Tsao, C.W. Polymer microfluidics: Simple, low-cost fabrication process bridging academic lab research to commercialized production. *Micromachines* **2016**, *7*, 225. [CrossRef] [PubMed]
66. Faustino, V.; Catarino, S.O.; Lima, R.; Minas, G. Biomedical microfluidic devices by using low-cost fabrication techniques: A review. *J. Biomech.* **2016**, *49*, 2280–2292. [CrossRef] [PubMed]
67. Focke, M.; Stumpf, F.; Faltin, B.; Reith, P.; Bamarni, D.; Wadle, S.; Müller, C.; Reinecke, H.; Schrenzel, J.; Francois, P.; et al. Microstructuring of polymer films for sensitive genotyping by real-time PCR on a centrifugal microfluidic platform. *Lab Chip* **2010**, *10*, 2519–2526. [CrossRef]
68. Xia, Y.; Whitesides, G.M. Soft lithography. *Angew. Chem. Int. Ed.* **1998**, *37*, 550–575. [CrossRef]
69. Mcdonald, J.C.; Duffy, D.C.; Anderson, J.R.; Chiu, D.T. Review General Fabrication of microfluidic systems in poly (dimethylsiloxane). *Electrophoresis* **2000**, *21*, 27–40. [CrossRef]
70. Kricka, L.J.; Fortina, P.; Panaro, N.J.; Wilding, P.; Alonso-Amigo, G.; Becker, H. Fabrication of plastic microchips by hot embossing. *Lab Chip* **2002**, *2*, 1–4. [CrossRef]
71. Chen, Y. Applications of nanoimprint lithography/hot embossing: A review. *Appl. Phys. Mater. Sci. Process.* **2015**, *121*, 451–465. [CrossRef]
72. Attia, U.M.; Marson, S.; Alcock, J.R. Micro-injection moulding of polymer microfluidic devices. *Microfluid. Nanofluid.* **2009**, *7*, 1. [CrossRef]
73. Juang, Y.J.; Lee, L.J.; Koelling, K.W. Hot embossing in microfabrication. Part I: Experimental. *Polym. Eng. Sci.* **2002**, *42*, 539–550. [CrossRef]
74. Chou, S.Y.; Krauss, P.R. Imprint lithography with sub-10 nm feature size and high throughput. *Microelectron. Eng.* **1997**, *35*, 237–240. [CrossRef]
75. Koerner, T.; Brown, L.; Xie, R.; Oleschuk, R.D. Epoxy resins as stamps for hot embossing of microstructures and microfluidic channels. *Sens. Actuators B Chem.* **2005**, *107*, 632–639. [CrossRef]
76. Goral, V.N.; Hsieh, Y.C.; Petzold, O.N.; Faris, R.A.; Yuen, P.K. Hot embossing of plastic microfluidic devices using poly (dimethylsiloxane) molds. *J. Micromech. Microeng.* **2010**, *21*, 017002. [CrossRef]
77. Ho, C.M.B.; Ng, S.H.; Li, K.H.H.; Yoon, Y.J. 3D printed microfluidics for biological applications. *Lab Chip* **2015**, *15*, 3627–3637. [CrossRef]
78. Chen, C.; Mehl, B.T.; Munshi, A.S.; Townsend, A.D.; Spence, D.M.; Martin, R.S. 3D-printed microfluidic devices: Fabrication, advantages and limitations—A mini review. *Anal. Methods* **2016**, *8*, 6005–6012. [CrossRef]
79. Butler, J.E. Solid supports in enzyme-linked immunosorbent assay and other solid-phase immunoassays. *Methods* **2000**, *22*, 4–23. [CrossRef]
80. Bai, Y.; Koh, C.G.; Boreman, M.; Juang, Y.J.; Tang, I.C.; Lee, L.J.; Yang, S.T. Surface modification for enhancing antibody binding on polymer-based microfluidic device for enzyme-linked immunosorbent assay. *Langmuir* **2006**, *22*, 9458–9467. [CrossRef]
81. Gray, J.J. The interaction of proteins with solid surfaces. *Curr. Opin. Struct. Biol.* **2004**, *14*, 110–115. [CrossRef]
82. Lai, J.; Sunderland, B.; Xue, J.; Yan, S.; Zhao, W.; Folkard, M.; Michael, B.D.; Wang, Y. Study on hydrophilicity of polymer surfaces improved by plasma treatment. *Appl. Surf. Sci.* **2006**, *252*, 3375–3379. [CrossRef]
83. Laib, S.; MacCraith, B.D. Immobilization of biomolecules on cycloolefin polymer supports. *Anal. Chem.* **2007**, *79*, 6264–6270. [CrossRef]
84. Yuan, Y.; He, H.; Lee, L.J. Protein a-based antibody immobilization onto polymeric microdevices for enhanced sensitivity of enzyme-linked immunosorbent assay. *Biotechnol. Bioeng.* **2009**, *102*, 891–901. [CrossRef] [PubMed]

85. Miyazaki, C.; Mishra, R.; Kinahan, D.; Ferreira, M.; Ducrée, J. Polyethylene imine/graphene oxide layer-by-layer surface functionalization for significantly improved limit of detection and binding kinetics of immunoassays on acrylate surfaces. *Colloids Surf. B Biointerfaces* **2017**, *158*. [CrossRef] [PubMed]
86. Nwankire, C.E.; Venkatanarayanan, A.; Glennon, T.; Keyes, T.E.; Forster, R.J.; Ducrée, J. Label-free impedance detection of cancer cells from whole blood on an integrated centrifugal microfluidic platform. *Biosens. Bioelectron.* **2015**, *68*, 382–389. [CrossRef] [PubMed]
87. Miyazaki, C.M.; Kinahan, D.J.; Mishra, R.; Mangwanya, F.; Kilcawley, N.; Ferreira, M.; Ducrée, J. Label-free, spatially multiplexed SPR detection of immunoassays on a highly integrated centrifugal Lab-on-a-Disc platform. *Biosens. Bioelectron.* **2018**, *119*, 86–93. [CrossRef]
88. Riegger, L.; Grumann, M.; Nann, T.; Riegler, J.; Ehlert, O.; Bessler, W.; Mittenbuehler, K.; Urban, G.; Pastewka, L.; Brenner, T.; et al. Read-out concepts for multiplexed bead-based fluorescence immunoassays on centrifugal microfluidic platforms. *Sens. Actuators A Phys.* **2006**, *126*, 455–462. [CrossRef]
89. Lim, C.T.; Zhang, Y. Bead-based microfluidic immunoassays: The next generation. *Biosens. Bioelectron.* **2007**, *22*, 1197–1204. [CrossRef]
90. Li, L.; Miao, B.; Li, Z.; Sun, Z.; Peng, N. Sample-to-Answer Hepatitis B Virus DNA Detection from Whole Blood on a Centrifugal Microfluidic Platform with Double Rotation Axes. *ACS Sens.* **2019**, *4*, 2738–2745. [CrossRef]
91. Koh, C.Y.; Schaff, U.Y.; Piccini, M.E.; Stanker, L.H.; Cheng, L.W.; Ravichandran, E.; Singh, B.R.; Sommer, G.J.; Singh, A.K. Centrifugal microfluidic platform for ultrasensitive detection of botulinum toxin. *Anal. Chem.* **2015**, *87*, 922–928. [CrossRef]
92. Lee, B.S.; Lee, J.N.; Park, J.M.; Lee, J.G.; Kim, S.; Cho, Y.K.; Ko, C. A fully automated immunoassay from whole blood on a disc. *Lab Chip* **2009**, *9*, 1548–1555. [CrossRef]
93. Honda, N.; Lindberg, U.; Andersson, P.; Hoffmann, S.; Takei, H. Simultaneous Multiple Immunoassays in a Compact Disc—Shaped Microfluidic Device Based on Centrifugal Force. *Clin. Chem.* **2005**, *51*, 1955–1961. [CrossRef]
94. Van Oordt, T.; Barb, Y.; Smetana, J.; Zengerle, R.; Von Stetten, F. Miniature stick-packaging-an industrial technology for pre-storage and release of reagents in lab-on-a-chip systems. *Lab Chip* **2013**, *13*, 2888–2892. [CrossRef] [PubMed]
95. Stumpf, F.; Schwemmer, F.; Hutzenlaub, T.; Baumann, D.; Strohmeier, O.; Dingemanns, G.; Simons, G.; Sager, C.; Plobner, L.; Von Stetten, F.; et al. LabDisk with complete reagent prestorage for sample-to-answer nucleic acid based detection of respiratory pathogens verified with influenza A H3N2 virus. *Lab Chip* **2016**, *16*, 199–207. [CrossRef] [PubMed]
96. Hoffmann, J.; Mark, D.; Lutz, S.; Zengerle, R.; von Stetten, F. Pre-storage of liquid reagents in glass ampoules for DNA extraction on a fully integrated lab-on-a-chip cartridge. *Lab Chip* **2010**, *10*, 1480–1484. [CrossRef] [PubMed]
97. Kazemzadeh, A.; Eriksson, A.; Madou, M.; Russom, A. A micro-dispenser for long-term storage and controlled release of liquids. *Nat. Commun.* **2019**, *10*, 1–11. [CrossRef] [PubMed]
98. Nwankire, C.E.; Chan, D.S.S.; Gaughran, J.; Burger, R.; Gorkin, R.; Ducrée, J. Fluidic Automation of Nitrate and Nitrite Bioassays in Whole Blood by Dissolvable-Film Based Centrifugo-Pneumatic Actuation. *Sensors* **2013**, *13*, 11336–11349. [CrossRef]
99. Mishra, R.; Zapatero-Rodríguez, J.; Sharma, S.; Kelly, D.; McAuley, D.; Gilgunn, S.; O'Kennedy, R.; Ducrée, J. Automation of multi-analyte prostate cancer biomarker immunoassay panel from whole blood by minimum-instrumentation rotational flow control. *Sens. Actuators B Chem.* **2018**, *263*, 668–675. [CrossRef]
100. Kuo, J.N.; Chen, X.F. Plasma separation and preparation on centrifugal microfluidic disk for blood assays. *Microsyst. Technol.* **2015**, *21*, 2485–2494. [CrossRef]
101. Kuo, J.N.; Chen, X.F. Decanting and mixing of supernatant human blood plasma on centrifugal microfluidic platform. *Microsyst. Technol.* **2016**, *22*, 861–869. [CrossRef]
102. Lin, C.H.; Shih, C.H.; Lu, C.H. A fully integrated prothrombin time test on the microfluidic disk analyzer. *J. Nanosci. Nanotechnol.* **2013**, *13*, 2206–2212. [CrossRef]
103. Lin, C.H.; Lin, K.W.; Yen, D.; Shih, C.H.; Lu, C.H.; Wang, J.M.; Lin, C.Y. A point-of-care prothrombin time test on a microfluidic disk analyzer using alternate spinning. *J. Nanosci. Nanotechnol.* **2015**, *15*, 1401–1407. [CrossRef]

104. Park, J.M.; Kim, M.S.; Moon, H.S.; Yoo, C.E.; Park, D.; Kim, Y.J.; Han, K.Y.; Lee, J.Y.; Oh, J.H.; Kim, S.S.; et al. Fully automated circulating tumor cell isolation platform with large-volume capacity based on lab-on-a-disc. *Anal. Chem.* **2014**, *86*, 3735–3742. [CrossRef] [PubMed]
105. Kim, T.H.; Hwang, H.; Gorkin, R.; Madou, M.; Cho, Y.K. Geometry effects on blood separation rate on a rotating disc. *Sens. Actuators B Chem.* **2013**, *178*, 648–655. [CrossRef]
106. Boycott, A. Sedimentation of blood corpuscles. *Nature* **1920**, *104*, 532–532. [CrossRef]
107. Agarwal, R.; Sarkar, A.; Chakraborty, S. Interplay of Coriolis effect with rheology results in unique blood dynamics on a compact disc. *Analyst* **2019**, *144*, 3782–3789. [CrossRef] [PubMed]
108. Kinahan, D.J.; Kearney, S.M.; Glynn, M.T.; Ducrée, J. Spira mirabilis enhanced whole blood processing in a lab-on-a-disk. *Sens. Actuators A Phys.* **2014**, *215*, 71–76. [CrossRef]
109. Yu, Z.T.F.; Joseph, J.G.; Liu, S.X.; Cheung, M.K.; Haffey, P.J.; Kurabayashi, K.; Fu, J. Centrifugal microfluidics for sorting immune cells from whole blood. *Sens. Actuators B Chem.* **2017**, *245*, 1050–1061. [CrossRef] [PubMed]
110. Uddin, R.; Donolato, M.; Hwu, E.T.; Hansen, M.F.; Boisen, A. Combined detection of C-reactive protein and PBMC quantification from whole blood in an integrated lab-on-a-disc microfluidic platform. *Sens. Actuators B Chem.* **2018**, *272*, 634–642. [CrossRef]
111. Glynn, M.; Kirby, D.; Chung, D.; Kinahan, D.J.; Kijanka, G.; Ducrée, J. Centrifugo-magnetophoretic purification of CD4+ cells from whole blood toward future HIV/AIDS point-of-care applications. *J. Lab. Autom.* **2014**, *19*, 285–296. [CrossRef]
112. Moen, S.T.; Hatcher, C.L.; Singh, A.K. A Centrifugal Microfluidic Platform That Separates Whole Blood Samples into Multiple Removable Fractions Due to Several Discrete but Continuous Density Gradient Sections. *PLoS ONE* **2016**, *11*, e0153137. [CrossRef]
113. Morijiri, T.; Yamada, M.; Hikida, T.; Seki, M. Microfluidic counterflow centrifugal elutriation system for sedimentation-based cell separation. *Microfluid. Nanofluid.* **2013**, *14*, 1049–1057. [CrossRef]
114. Tefferi, A.; Hanson, C.A.; Inwards, D.J. How to interpret and pursue an abnormal complete blood cell count in adults. *Mayo Clin. Proc.* **2005**, *80*, 923–936. [CrossRef] [PubMed]
115. Park, J.M.; Lee, J.Y.; Lee, J.G.; Jeong, H.; Oh, J.M.; Kim, Y.J.; Park, D.; Kim, M.S.; Lee, H.J.; Oh, J.H.; et al. Highly efficient assay of circulating tumor cells by selective sedimentation with a density gradient medium and microfiltration from whole blood. *Anal. Chem.* **2012**, *84*, 7400–7407. [CrossRef] [PubMed]
116. Lim, M.; Park, J.; Lowe, A.C.; Jeong, H.o.; Lee, S.; Park, H.C.; Lee, K.; Kim, G.H.; Kim, M.H.; Cho, Y.K. A lab-on-a-disc platform enables serial monitoring of individual CTCs associated with tumor progression during EGFR-targeted therapy for patients with NSCLC. *Theranostics* **2020**, *10*, 5181. [CrossRef] [PubMed]
117. Kim, C.J.; Ki, D.Y.; Park, J.; Sunkara, V.; Kim, T.H.; Min, Y.; Cho, Y.K. Fully automated platelet isolation on a centrifugal microfluidic device for molecular diagnostics. *Lab Chip* **2020**, *20*, 949–957. [CrossRef] [PubMed]
118. Schaff, U.Y.; Sommer, G.J. Whole blood immunoassay based on centrifugal bead sedimentation. *Clin. Chem.* **2011**, *57*, 753–761. [CrossRef] [PubMed]
119. Mark, D.; Weber, P.; Lutz, S.; Focke, M.; Zengerle, R.; von Stetten, F. Aliquoting on the centrifugal microfluidic platform based on centrifugo-pneumatic valves. *Microfluid. Nanofluid.* **2011**, *10*, 1279–1288. [CrossRef]
120. Mark, D.; Metz, T.; Haeberle, S.; Lutz, S.; Ducrée, J.; Zengerle, R.; von Stetten, F. Centrifugo-pneumatic valve for metering of highly wetting liquids on centrifugal microfluidic platforms. *Lab Chip* **2009**, *9*, 3599–3603. [CrossRef] [PubMed]
121. Kim, T.H.; Kim, C.J.; Kim, Y.; Cho, Y.K. Centrifugal microfluidic system for a fully automated N-fold serial dilution. *Sens. Actuators B Chem.* **2018**, *256*, 310–317. [CrossRef]
122. Ducrée, J.; Brenner, T.; Haeberle, S.; Glatzel, T.; Zengerle, R. Multilamination of flows in planar networks of rotating microchannels. *Microfluid. Nanofluid.* **2006**, *2*, 78–84. [CrossRef]
123. Ducrée, J.; Haeberle, S.; Brenner, T.; Glatzel, T.; Zengerle, R. Patterning of flow and mixing in rotating radial microchannels. *Microfluid. Nanofluid.* **2006**, *2*, 97–105. [CrossRef]
124. Grumann, M.; Geipel, A.; Riegger, L.; Zengerle, R.; Ducrée, J. Batch-mode mixing on centrifugal microfluidic platforms. *Lab Chip* **2005**, *5*, 560–565. [CrossRef] [PubMed]
125. Park, S.J.; Kim, J.K.; Park, J.; Chung, S.; Chung, C.; Chang, J.K. Rapid three-dimensional passive rotation micromixer using the breakup process. *J. Micromech. Microeng.* **2003**, *14*, 6. [CrossRef]
126. Park, J.; Lee, G.H.; Park, J.Y.; Lee, J.C.; Kim, H.C. A numerical study of the Coriolis effect in centrifugal microfluidics with different channel arrangements. *Microfluid. Nanofluid.* **2016**, *20*, 65. [CrossRef]

127. Cai, Z.; Xiang, J.; Chen, H.; Wang, W. A Rapid Micromixer for Centrifugal Microfluidic Platforms. *Micromachines* **2016**, *7*, 89. [CrossRef] [PubMed]
128. Rida, A.; Lehnert, T.; Gijs, M. Microfluidic mixer using magnetic beads. In Proceedings of the 7th International Conference on Miniaturized Chemical and Biochemical Analysis Systems, Squaw Valley, California, 5–9 October 2003; pp. 579–582.
129. Burger, R.; Reith, P.; Akujobi, V.; Ducrée, J. Rotationally controlled magneto-hydrodynamic particle handling for bead-based microfluidic assays. *Microfluid. Nanofluid.* **2012**, *13*, 675–681. [CrossRef]
130. Hessel, V.; Löwe, H.; Schönfeld, F. Micromixers—A review on passive and active mixing principles. *Chem. Eng. Sci.* **2005**, *60*, 2479–2501. [CrossRef]
131. Noroozi, Z.; Kido, H.; Micic, M.; Pan, H.; Bartolome, C.; Princevac, M.; Zoval, J.; Madou, M. Reciprocating flow-based centrifugal microfluidics mixer. *Rev. Sci. Instrum.* **2009**, *80*. [CrossRef] [PubMed]
132. Noroozi, Z.; Kido, H.; Peytavi, R.; Nakajima-Sasaki, R.; Jasinskas, A.; Micic, M.; Felgner, P.L.; Madou, M.J. A multiplexed immunoassay system based upon reciprocating centrifugal microfluidics. *Rev. Sci. Instruments* **2011**, *82*. [CrossRef]
133. Hess, J.; Zehnle, S.; Juelg, P.; Hutzenlaub, T.; Zengerle, R.; Paust, N. Review on pneumatic operations in centrifugal microfluidics. *Lab Chip* **2019**, *19*, 3745–3770. [CrossRef]
134. Aeinehvand, M.M.; Ibrahim, F.; Al-Faqheri, W.; Thio, T.H.G.; Kazemzadeh, A.; Madou, M. Latex micro-balloon pumping in centrifugal microfluidic platforms. *Lab Chip* **2014**, *14*, 988–997. [CrossRef]
135. Clime, L.; Brassard, D.; Geissler, M.; Veres, T. Active pneumatic control of centrifugal microfluidic flows for lab-on-a-chip applications. *Lab Chip* **2015**, *15*, 2400–2411. [CrossRef]
136. Burger, S.; Schulz, M.; von Stetten, F.; Zengerle, R.; Paust, N. Rigorous buoyancy driven bubble mixing for centrifugal microfluidics. *Lab Chip* **2016**, *16*, 261–268. [CrossRef] [PubMed]
137. Czilwik, G.; Messinger, T.; Strohmeier, O.; Wadle, S.; Von Stetten, F.; Paust, N.; Roth, G.; Zengerle, R.; Saarinen, P.; Niittymäki, J.; et al. Rapid and fully automated bacterial pathogen detection on a centrifugal-microfluidic LabDisk using highly sensitive nested PCR with integrated sample preparation. *Lab Chip* **2015**, *15*, 3749–3759. [CrossRef] [PubMed]
138. Seo, J.H.; Park, B.H.; Oh, S.J.; Choi, G.; Kim, D.H.; Lee, E.Y.; Seo, T.S. Development of a high-throughput centrifugal loop-mediated isothermal amplification microdevice for multiplex foodborne pathogenic bacteria detection. *Sens. Actuators B Chem.* **2017**, *246*, 146–153. [CrossRef]
139. Loo, J.; Kwok, H.; Leung, C.; Wu, S.; Law, I.; Cheung, Y.; Cheung, Y.; Chin, M.; Kwan, P.; Hui, M.; et al. Sample-to-answer on molecular diagnosis of bacterial infection using integrated lab-on-a-disc. *Biosens. Bioelectron.* **2017**, *93*, 212–219. [CrossRef] [PubMed]
140. Lim, D.Y.S.; Seo, M.J.; Yoo, J.C. Optical Temperature Control Unit and Convolutional Neural Network for Colorimetric Detection of Loop-Mediated Isothermal Amplification on a Lab-On-A-Disc Platform. *Sensors* **2019**, *19*, 3207. [CrossRef] [PubMed]
141. Sayad, A.; Ibrahim, F.; Uddin, S.M.; Cho, J.; Madou, M.; Thong, K.L. A microdevice for rapid, monoplex and colorimetric detection of foodborne pathogens using a centrifugal microfluidic platform. *Biosens. Bioelectron.* **2018**, *100*, 96–104. [CrossRef]
142. Brennan, D.; Coughlan, H.; Clancy, E.; Dimov, N.; Barry, T.; Kinahan, D.; Ducrée, J.; Smith, T.J.; Galvin, P. Development of an on-disc isothermal in vitro amplification and detection of bacterial RNA. *Sens. Actuators B Chem.* **2017**, *239*, 235–242. [CrossRef]
143. Schuler, F.; Schwemmer, F.; Trotter, M.; Wadle, S.; Zengerle, R.; von Stetten, F.; Paust, N. Centrifugal step emulsification applied for absolute quantification of nucleic acids by digital droplet RPA. *Lab Chip* **2015**, *15*, 2759–2766. [CrossRef]
144. Lutz, S.; Weber, P.; Focke, M.; Faltin, B.; Hoffmann, J.; Müller, C.; Mark, D.; Roth, G.; Munday, P.; Armes, N.; et al. Microfluidic lab-on-a-foil for nucleic acid analysis based on isothermal recombinase polymerase amplification (RPA). *Lab Chip* **2010**, *10*, 887–893. [CrossRef]
145. Antunes, P.; Watterson, D.; Parmvi, M.; Burger, R.; Boisen, A.; Young, P.; Cooper, M.A.; Hansen, M.F.; Ranzoni, A.; Donolato, M. Quantification of NS1 dengue biomarker in serum via optomagnetic nanocluster detection. *Sci. Rep.* **2015**, *5*, 16145. [CrossRef] [PubMed]
146. Uddin, R.; Burger, R.; Donolato, M.; Fock, J.; Creagh, M.; Hansen, M.F.; Boisen, A. Lab-on-a-disc agglutination assay for protein detection by optomagnetic readout and optical imaging using nano- and micro-sized magnetic beads. *Biosens. Bioelectron.* **2016**, *85*, 351–357. [CrossRef]

147. Steigert, J.; Grumann, M.; Dube, M.; Streule, W.; Riegger, L.; Brenner, T.; Koltay, P.; Mittmann, K.; Zengerle, R.; Ducrée, J. Direct hemoglobin measurement on a centrifugal microfluidic platform for point-of-care diagnostics. *Sens. Actuators A Phys.* **2006**, *130–131*, 228–233. [CrossRef]
148. Grumann, M.; Steigert, J.; Riegger, L.; Moser, I.; Enderle, B.; Riebeseel, K.; Urban, G.; Zengerle, R.; Ducrée, J. Sensitivity enhancement for colorimetric glucose assays on whole blood by on-chip beam-guidance. *Biomed. Microdevices* **2006**, *8*, 209–214. [CrossRef] [PubMed]
149. Ukita, Y.; Takamura, Y. A new stroboscopic technique for the observation of microscale fluorescent objects on a spinning platform in centrifugal microfluidics. *Microfluid. Nanofluid.* **2014**, *18*, 245–252. [CrossRef]
150. Piruska, A.; Nikcevic, I.; Lee, S.H.; Ahn, C.; Heineman, W.R.; Limbach, P.A.; Seliskar, C.J. The autofluorescence of plastic materials and chips measured under laser irradiation. *Lab Chip* **2005**, *5*, 1348–1354. [CrossRef] [PubMed]
151. Hemmi, A.; Usui, T.; Moto, A.; Tobita, T.; Soh, N.; Nakano, K.; Zeng, H.; Uchiyama, K.; Imato, T.; Nakajima, H. A surface plasmon resonance sensor on a compact disk-type microfluidic device. *J. Sep. Sci.* **2011**, *34*, 2913–2919. [CrossRef]
152. Rattanarat, P.; Teengam, P.; Siangproh, W.; Ishimatsu, R.; Nakano, K.; Chailapakul, O.; Imato, T. An electrochemical compact disk-type microfluidics platform for use as an enzymatic biosensor. *Electroanalysis* **2015**, *27*, 703–712. [CrossRef]
153. Rajendran, S.T.; Scarano, E.; Bergkamp, M.H.; Capria, A.M.; Cheng, C.H.; Sanger, K.; Ferrari, G.; Nielsen, L.H.; Hwu, E.T.; Zor, K.; et al. Modular, lightweight, wireless potentiostat-on-a-disc for electrochemical detection in centrifugal microfluidics. *Anal. Chem.* **2019**, *91*, 11620–11628. [CrossRef]
154. Czugala, M.; Maher, D.; Collins, F.; Burger, R.; Hopfgartner, F.; Yang, Y.; Zhaou, J.; Ducrée, J.; Smeaton, A.; Fraser, K.J.; et al. CMAS: Fully integrated portable centrifugal microfluidic analysis system for on-site colorimetric analysis. *RSC Adv.* **2013**, *3*, 15928–15938. [CrossRef]
155. Jung, J.H.; Park, B.H.; Oh, S.J.; Choi, G.; Seo, T.S. Integrated centrifugal reverse transcriptase loop-mediated isothermal amplification microdevice for influenza A virus detection. *Biosens. Bioelectron.* **2015**, *68*, 218–224. [CrossRef] [PubMed]
156. Chang, H.C.; Chao, Y.T.; Yen, J.Y.; Yu, Y.L.; Lee, C.N.; Ho, B.C.; Liu, K.C.; Fang, J.; Lin, C.W.; Lee, J.H. A Turbidity Test Based Centrifugal Microfluidics Diagnostic System for Simultaneous Detection of HBV, HCV, and CMV. *Adv. Mater. Sci. Eng.* **2015**, *2015*. [CrossRef]
157. Liu, Q.; Zhang, X.; Chen, L.; Yao, Y.; Ke, S.; Zhao, W.; Yang, Z.; Sui, G. A sample-to-answer labdisc platform integrated novel membrane-resistance valves for detection of highly pathogenic avian influenza viruses. *Sens. Actuators B Chem.* **2018**, *270*, 371–381. [CrossRef]
158. Miao, B.; Peng, N.; Li, L.; Li, Z.; Hu, F.; Zhang, Z.; Wang, C. Centrifugal Microfluidic System for Nucleic Acid Amplification and Detection. *Sensors* **2015**, *15*, 27954–27968. [CrossRef]
159. Amasia, M.; Cozzens, M.; Madou, M.J. Centrifugal microfluidic platform for rapid PCR amplification using integrated thermoelectric heating and ice-valving. *Sens. Actuators B Chem.* **2012**, *161*, 1191–1197. [CrossRef]
160. Sayad, A.A.; Ibrahim, F.; Uddin, S.M.; Pei, K.X.; Mohktar, M.S.; Madou, M.; Thong, K.L. A microfluidic lab-on-a-disc integrated loop mediated isothermal amplification for foodborne pathogen detection. *Sens. Actuators B Chem.* **2016**, *227*, 600–609. [CrossRef]
161. Thiha, A.; Ibrahim, F. A Colorimetric Enzyme-Linked Immunosorbent Assay (ELISA) Detection Platform for a Point-of-Care Dengue Detection System on a Lab-on-Compact-Disc. *Sensors* **2015**, *15*, 11431–11441. [CrossRef] [PubMed]
162. Nwankire, C.E.; Donohoe, G.G.; Zhang, X.; Siegrist, J.; Somers, M.; Kurzbuch, D.; Monaghan, R.; Kitsara, M.; Burger, R.; Hearty, S.; et al. At-line bioprocess monitoring by immunoassay with rotationally controlled serial siphoning and integrated supercritical angle fluorescence optics. *Anal. Chim. Acta* **2013**, *781*, 54–62. [CrossRef]
163. Oh, S.J.; Park, B.H.; Jung, J.H.; Choi, G.; Lee, D.C.; Seo, T.S. Centrifugal loop-mediated isothermal amplification microdevice for rapid, multiplex and colorimetric foodborne pathogen detection. *Biosens. Bioelectron.* **2016**, *75*, 293–300. [CrossRef]
164. Mahmodi Arjmand, E.; Saadatmand, M.; Bakhtiari, M.R.; Eghbal, M. Design and fabrication of a centrifugal microfluidic disc including septum valve for measuring hemoglobin A1c in human whole blood using immunoturbidimetry method. *Talanta* **2018**, *190*, 134–139. [CrossRef]

165. Miyazaki, C.M.; Shimizu, F.M.; Ferreira, M. Surface plasmon resonance (SPR) for sensors and biosensors. In *Nanocharacterization Techniques*; Elsevier: Amsterdam, The Netherlands, 2017; pp. 183–200.
166. Yih, J.N.; Chiu, K.C.; Chou, S.Y.; Lin, C.M.; Lan, Y.S.; Chen, S.J.; Cheng, N.J. Surface plasmon resonance biosensor based on grating disc with circular fluidic channel. In Proceedings of the 2011 6th IEEE International Conference on Nano/Micro Engineered and Molecular Systems, Kaohsiung, Taiwan, 20–23 February 2011; pp. 571–574.
167. Biosurfit. Biosurfit. Available online: https://www.biosurfit.com/en/ (accessed on 26 May 2020).
168. Martin, J.; Nieuwoudt, M.; Vargas, M.; Bodley, O.; Yohendiran, T.; Oosterbeek, R.; Williams, D.; Simpson, M.C. Raman on a disc: High-quality Raman spectroscopy in an open channel on a centrifugal microfluidic disc. *Analyst* **2017**, *142*, 1682–1688. [CrossRef] [PubMed]
169. Choi, D.; Kang, T.; Cho, H.; Choi, Y.; Lee, L.P. Additional amplifications of SERS via an optofluidic CD-based platform. *Lab Chip* **2009**, *9*, 239–243. [CrossRef]
170. Morelli, L.; Serioli, L.; Centorbi, F.A.; Jendresen, C.B.; Matteucci, M.; Ilchenko, O.; Demarchi, D.; Nielsen, A.T.; Zór, K.; Boisen, A. Injection molded lab-on-a-disc platform for screening of genetically modified E. coli using liquid–liquid extraction and surface enhanced Raman scattering. *Lab Chip* **2018**, *18*, 869–877. [CrossRef] [PubMed]
171. Fan, M.; Andrade, G.F.; Brolo, A.G. A review on recent advances in the applications of surface-enhanced Raman scattering in analytical chemistry. *Anal. Chim. Acta* **2020**, *1097*, 1–29. [CrossRef] [PubMed]
172. Okamoto, S.; Ukita, Y. Automatic microfluidic enzyme-linked immunosorbent assay based on CLOCK-controlled autonomous centrifugal microfluidics. *Sens. Actuators B Chem.* **2018**, *261*, 264–270. [CrossRef]
173. Nwankire, C.E.; Czugala, M.; Burger, R.; Fraser, K.J.; O'Connell, T.M.; Glennon, T.; Onwuliri, B.E.; Nduaguibe, I.E.; Diamond, D.; Ducrée, J.; et al. A portable centrifugal analyser for liver function screening. *Biosens. Bioelectron.* **2014**, *56*, 352–358. [CrossRef] [PubMed]
174. Wang, K.; Liang, R.; Chen, H.; Lu, S.; Jia, S.; Wang, W. A microfluidic immunoassay system on a centrifugal platform. *Sens. Actuators B Chem.* **2017**, *251*, 242–249. [CrossRef]
175. Lee, W.S.; Sunkara, V.; Han, J.R.; Park, Y.S.; Cho, Y.K. Electrospun TiO 2 nanofiber integrated lab-on-a-disc for ultrasensitive protein detection from whole blood. *Lab Chip* **2015**, *15*, 478–485. [CrossRef]
176. Thio, T.H.G.; Ibrahim, F.; Al-Faqheri, W.; Soin, N.; Bador, M.K.; Madou, M. Sequential push-pull pumping mechanism for washing and evacuation of an immunoassay reaction chamber on a microfluidic CD platform. *PLoS ONE* **2015**, *10*, e0121836. [CrossRef]
177. Sanger, K.; Zor, K.; Jendresen, C.B.; Heiskanen, A.; Amato, L.; Nielsen, A.T.; Boisen, A. Lab-on-a-disc platform for screening of genetically modified E. coli cells via cell-free electrochemical detection of p-Coumaric acid. *Sens. Actuators B Chem.* **2017**, *253*, 999–1005. [CrossRef]
178. Yoon, Y.J.; Li, K.H.H.; Low, Y.Z.; Yoon, J.; Ng, S.H. Microfluidics biosensor chip with integrated screen-printed electrodes for amperometric detection of nerve agent. *Sens. Actuators B Chem.* **2014**, *198*, 233–238. [CrossRef]
179. Ronkainen, N.J.; Halsall, H.B.; Heineman, W.R. Electrochemical biosensors. *Chem. Soc. Rev.* **2010**, *39*, 1747–1763. [CrossRef] [PubMed]
180. Li, T.; Fan, Y.; Cheng, Y.; Yang, J. An electrochemical Lab-on-a-CD system for parallel whole blood analysis. *Lab Chip* **2013**, *13*, 2634–2640. [CrossRef] [PubMed]
181. Abi-Samra, K.; Kim, T.H.; Park, D.K.; Kim, N.; Kim, J.; Kim, H.; Cho, Y.K.; Madou, M. Electrochemical velocimetry on centrifugal microfluidic platforms. *Lab Chip* **2013**, *13*, 3253–3260. [CrossRef] [PubMed]
182. Abaxis, I. Piccolo Xpress. Available online: https://www.abaxis.com/medical/piccolo-xpress (accessed on 29 May 2020).
183. Bioscience, M. Revogene. Available online: https://www.meridianbioscience.com/platform/molecular/revogene (accessed on 29 May 2020).
184. DiaSorin Group, I. Simplexa. Available online: https://www.focusdx.com/integrated-cycler/dad-intl (accessed on 1 June 2020).
185. Hahn-Schickard. Hahn-Schickard. Available online: https://www.hahn-schickard.de/en/ (accessed on 27 May 2020).
186. Nguyen, T.; Duong Bang, D.; Wolff, A. 2019 novel coronavirus disease (COVID-19): paving the road for rapid detection and point-of-care diagnostics. *Micromachines* **2020**, *11*, 306. [CrossRef]
187. GmbH, S. Spindiag. Available online: https://www.spindiag.de/ (accessed on 4 June 2020).

188. Dysinger, M.; Ma, M. A Gyrolab Assay for the Quantitation of Free Complement Protein C5a in Human Plasma. *AAPS J.* **2018**, *20*, 106. [CrossRef]
189. Ghosh, J.G.; Nguyen, A.A.; Bigelow, C.E.; Poor, S.; Qiu, Y.; Rangaswamy, N.; Ornberg, R.; Jackson, B.; Mak, H.; Ezell, T.; et al. Long-acting protein drugs for the treatment of ocular diseases. *Nat. Commun.* **2017**, *8*, 14837. [CrossRef]
190. Zhu, L.; Wang, Y.; Joyce, A.; Djura, I.; Gorovits, B. Fit-for-purpose validation of a ligand binding assay for toxicokinetic study using mouse serial sampling. *Pharm. Res.* **2019**, *36*, 169. [CrossRef]
191. Lee, B.S.; Lee, Y.U.; Kim, H.S.; Kim, T.H.; Park, J.; Lee, J.G.; Kim, J.; Kim, H.; Lee, W.G.; Cho, Y.K. Fully integrated lab-on-a-disc for simultaneous analysis of biochemistry and immunoassay from whole blood. *Lab Chip* **2011**, *11*, 70–78. [CrossRef]
192. Liao, T.; Wang, X.; Donolato, M.; Harris, E.; Cruz, M.M.; Balmaseda, A.; Wang, R.Y. Evaluation of ViroTrack Sero Zika IgG/IgM, a New Rapid and Quantitative Zika Serological Diagnostic Assay. *Diagnostics* **2020**, *10*, 372. [CrossRef]
193. Alejo-Cancho, I.; Navero-Castillejos, J.; Peiró-Mestres, A.; Albarracín, R.; Barrachina, J.; Navarro, A.; Gonzalo, V.; Pastor, V.; Muñoz, J.; Martínez, M.J. Evaluation of a novel microfluidic immuno-magnetic agglutination assay method for detection of dengue virus NS1 antigen. *PLoS Negl. Trop. Dis.* **2020**, *14*, e0008082. [CrossRef]
194. Keller, M.; Wadle, S.; Paust, N.; Dreesen, L.; Nuese, C.; Strohmeier, O.; Zengerle, R.; Von Stetten, F. Centrifugo-thermopneumatic fluid control for valving and aliquoting applied to multiplex real-time PCR on off-the-shelf centrifugal thermocycler. *RSC Adv.* **2015**, *5*, 89603–89611. [CrossRef]
195. Strohmeier, O.; Laßmann, S.; Riedel, B.; Mark, D.; Roth, G.; Werner, M.; Zengerle, R.; von Stetten, F. Multiplex genotyping of KRAS point mutations in tumor cell DNA by allele-specific real-time PCR on a centrifugal microfluidic disk segment. *Microchim. Acta* **2014**, *181*, 1681–1688. [CrossRef]
196. Choi, G.; Prince, T.; Miao, J.; Cui, L.; Guan, W. Sample-to-answer palm-sized nucleic acid testing device towards low-cost malaria mass screening. *Biosens. Bioelectron.* **2018**, *115*, 83–90. [CrossRef] [PubMed]
197. Huang, G.; Huang, Q.; Xie, L.; Xiang, G.; Wang, L.; Xu, H.; Ma, L.; Luo, X.; Xin, J.; Zhou, X.; et al. A rapid, low-cost, and microfluidic chip-based system for parallel identification of multiple pathogens related to clinical pneumonia. *Sci. Rep.* **2017**, *7*, 6441. [CrossRef] [PubMed]
198. Lee, A.; Park, J.; Lim, M.; Sunkara, V.; Kim, S.Y.; Kim, G.H.; Kim, M.H.; Cho, Y.K. All-in-one centrifugal microfluidic device for size-selective circulating tumor cell isolation with high purity. *Anal. Chem.* **2014**, *86*, 11349–11356. [CrossRef] [PubMed]
199. Kim, T.H.; Lim, M.; Park, J.; Oh, J.M.; Kim, H.; Jeong, H.; Lee, S.J.; Park, H.C.; Jung, S.; Kim, B.C.; et al. FAST: Size-selective, clog-free isolation of rare cancer cells from whole blood at a liquid–liquid interface. *Anal. Chem.* **2017**, *89*, 1155–1162. [CrossRef] [PubMed]
200. Clinomics Inc. Clinomics. Available online: http://clinomics.com/en/main (accessed on 28 May 2020).
201. Kim, H.; Lim, M.; Kim, J.Y.; Shin, S.J.; Cho, Y.K.; Cho, C.H. Circulating Tumor Cells Enumerated by a Centrifugal Microfluidic Device as a Predictive Marker for Monitoring Ovarian Cancer Treatment: A Pilot Study. *Diagnostics* **2020**, *10*, 249. [CrossRef]
202. Torres Delgado, S.M.; Kinahan, D.J.; Nirupa Julius, L.A.; Mallette, A.; Ardila, D.S.; Mishra, R.; Miyazaki, C.M.; Korvink, J.G.; Ducrée, J.; Mager, D. Wirelessly powered and remotely controlled valve-array for highly multiplexed analytical assay automation on a centrifugal microfluidic platform. *Biosens. Bioelectron.* **2018**, *109*, 214–223. [CrossRef]
203. Delgado, S.M.T.; Kinahan, D.J.; Sandoval, F.S.; Julius, L.A.N.; Kilcawley, N.A.; Ducrée, J.; Mager, D. Fully automated chemiluminescence detection using an electrified-Lab-on-a-Disc (eLoaD) platform. *Lab Chip* **2016**, *16*, 4002–4011. [CrossRef]
204. Delgado, S.M.T.; Korvink, J.G.; Mager, D. The eLoaD platform endows centrifugal microfluidics with on-disc power and communication. *Biosens. Bioelectron.* **2018**, *117*, 464–473. [CrossRef] [PubMed]
205. Bauer, M.; Bartoli, J.; Martinez-Chapa, S.O.; Madou, M. Wireless electrochemical detection on a microfluidic compact disc (CD) and evaluation of redox-amplification during flow. *Micromachines* **2019**, *10*, 31. [CrossRef] [PubMed]
206. Tavakoli, H.; Zhou, W.; Ma, L.; Perez, S.; Ibarra, A.; Xu, F.; Zhan, S.; Li, X. Recent advances in microfluidic platforms for single-cell analysis in cancer biology, diagnosis and therapy. *TrAC Trends Anal. Chem.* **2019**, *117*, 13–26. [CrossRef] [PubMed]

207. Dixon, C.; Ng, A.H.; Fobel, R.; Miltenburg, M.B.; Wheeler, A.R. An inkjet printed, roll-coated digital microfluidic device for inexpensive, miniaturized diagnostic assays. *Lab Chip* **2016**, *16*, 4560–4568. [CrossRef]
208. Hin, S.; Paust, N.; Keller, M.; Rombach, M.; Strohmeier, O.; Zengerle, R.; Mitsakakis, K. Temperature change rate actuated bubble mixing for homogeneous rehydration of dry pre-stored reagents in centrifugal microfluidics. *Lab Chip* **2018**, *18*, 362–370. [CrossRef]
209. Costantini, M.; Jaroszewicz, J.; Kozoń, Ł.; Szlązak, K.; Święszkowski, W.; Garstecki, P.; Stubenrauch, C.; Barbetta, A.; Guzowski, J. 3D-Printing of Functionally Graded Porous Materials Using On-Demand Reconfigurable Microfluidics. *Angew. Chem. Int. Ed.* **2019**, *58*, 7620–7625. [CrossRef]
210. Arango, Y.; Temiz, Y.; Gökçe, O.; Delamarche, E. Electrogates for stop-and-go control of liquid flow in microfluidics. *Appl. Phys. Lett.* **2018**, *112*, 153701. [CrossRef]
211. Alazzam, A.; Alamoodi, N. Microfluidic Devices with Patterned Wettability Using Graphene Oxide for Continuous Liquid–Liquid Two-Phase Separation. *ACS Appl. Nano Mater.* **2020**, *3*, 3471–3477. [CrossRef]
212. Wang, Y.; Toyoda, K.; Uesugi, K.; Morishima, K. A simple micro check valve using a photo-patterned hydrogel valve core. *Sens. Actuators A Phys.* **2020**, *304*, 111878. [CrossRef]
213. Van Nguyen, H.; Nguyen, V.D.; Nguyen, H.Q.; Chau, T.H.T.; Lee, E.Y.; Seo, T.S. Nucleic acid diagnostics on the total integrated lab-on-a-disc for point-of-care testing. *Biosens. Bioelectron.* **2019**, *141*, 111466. [CrossRef]
214. Brassard, D.; Geissler, M.; Descarreaux, M.; Tremblay, D.; Daoud, J.; Clime, L.; Mounier, M.; Charlebois, D.; Veres, T. Extraction of nucleic acids from blood: unveiling the potential of active pneumatic pumping in centrifugal microfluidics for integration and automation of sample preparation processes. *Lab Chip* **2019**, *19*, 1941–1952. [CrossRef] [PubMed]
215. Moeller, M.E.; Fock, J.; Pah, P.; Veras, A.D.L.C.; Bade, M.; Donolato, M.; Israelsen, S.B.; Eugen-Olsen, J.; Benfield, T.; Engsig, F.N. Evaluation of commercially available immuno-magnetic agglutination and enzyme-linked immunosorbent assays for rapid point-of-care diagnostics of COVID-19. *medRxiv* **2020**. [CrossRef]
216. Vasilescu, S.A.; Bazaz, S.R.; Jin, D.; Shimoni, O.; Warkiani, M.E. 3D printing enables the rapid prototyping of modular microfluidic devices for particle conjugation. *Appl. Mater. Today* **2020**, *20*, 100726. [CrossRef]
217. Mitxelena-Iribarren, O.; Zabalo, J.; Arana, S.; Mujika, M. Improved microfluidic platform for simultaneous multiple drug screening towards personalized treatment. *Biosens. Bioelectron.* **2019**, *123*, 237–243. [CrossRef]
218. Zhang, Y.; Xiang, J.; Wang, Y.; Qiao, Z.; Wang, W. A 3D printed centrifugal microfluidic platform for spilled oil enrichment and detection based on solid phase extraction (SPE). *Sens. Actuators B Chem.* **2019**, *296*, 126603. [CrossRef]
219. Weisgrab, G.; Ovsianikov, A.; Costa, P.F. Functional 3D printing for microfluidic chips. *Adv. Mater. Technol.* **2019**, *4*, 1900275. [CrossRef]
220. Bazaz, S.R.; Rouhi, O.; Raoufi, M.A.; Ejeian, F.; Asadnia, M.; Jin, D.; Warkiani, M.E. 3D Printing of Inertial Microfluidic Devices. *Sci. Rep.* **2020**, *10*, 1–14.
221. Carrell, C.; Kava, A.; Nguyen, M.; Menger, R.; Munshi, Z.; Call, Z.; Nussbaum, M.; Henry, C. Beyond the lateral flow assay: A review of paper-based microfluidics. *Microelectron. Eng.* **2019**, *206*, 45–54. [CrossRef]